PHARMACOKINETIC CHARACTERIZATION OF ANGIOTENSIN IV ANALOGS WITH THERAPEUTIC POTENTIAL FOR CANCER AND DEMENTIA.

By

ALENE MCCOY

A dissertation submitted in partial fulfillment of the requirements for the degree of

DOCTOR OF PHILOSOPHY

WASHINGTON STATE UNIVERSITY
Graduate Program in Pharmacology and Toxicology

MAY 2010

To the Faculty of Washington State University:

The members of the Committee appointed to examine the dissertation of ALENE MCCOY find it satisfactory and recommend that it be accepted.

Joseph W. Harding, Ph.D., Chair

John W. Wright, Ph.D.

Neal Davies, Ph.D.

Raymond Quock, Ph.D.

Heiko Jansen, Ph.D.

ACKNOWLEDGEMENTS

There are many people without whose support the research presented in this dissertation would not have been possible. First and foremost, I would like to thank my thesis advisor Joseph Harding for his professional and personal guidance and support throughout my graduate career. Your great generosity and wisdom will forever be an inspiration to me.

I would also like to thank my thesis committee and the faculty in the Program in Pharmacology and Toxicology. Thank you for always being available and for your professional guidance. Special thanks to Neal Davies for your generous assistance with all of my pharmacokinetic queries.

Thanks to all of the past employees of Pacific Northwest Biotechnology and to present members of the Harding laboratory. You made PNB and the Harding lab a wonderful place to work and taught me a great deal. I would especially like to acknowledge Brent Yamamoto who was a mentor to me during my first three years in graduate school, and my good friend Caroline Benoist. Your support and friendship have enriched both my personal and laboratory life.

PHARMACOKINETIC CHARACTERIZATION OF ANGIOTENSIN IV ANALOGS WITH THERAPEUTIC POTENTIAL FOR CANCER AND DEMENTIA

Abstract

By Alene McCoy, Ph.D.
Washington State University
May 2010

Chair: Joseph W. Harding

Angiotensin IV is a peptide hormone that acts via the AT_4 receptor with physiological functions that have not yet been fully elucidated but appear to include important roles in the processes of cognition, fluid balance, blood flow and vascular repair and remodeling. Angiotensin IV shares a partial homology with hepatocyte growth factor (HGF) and our laboratory has recently demonstrated that angiotensin IV analogs are able to effect changes in intracellular signaling cascades via the HGF receptor (c-Met). HGF/c-Met signaling is essential for embryonic development and is responsible for direction of cellular processes including differentiation, proliferation and migration. As the product of an oncogene, the c-Met receptor is also implicated to play a critical role cancer.

Our laboratory has developed a library of angiotensin IV analogs with a number of these exhibiting strong potential as therapeutic agents for the treatment of cancer or dementia. Given that the failure of many therapeutic candidates in clinical trials can be attributed to unsuitable pharmacokinetics, our laboratory wished to establish a basic understanding of the

pharmacokinetic characteristics of these molecules. We, therefore, set out to establish the basic pharmacokinetic profiles of three molecules, which serve as representative molecules for classes of chemical modifications to the angiotensin IV peptide made in our laboratory.

This dissertation presents results from *in-vitro* and *in-vivo* studies describing pharmacokinetic characteristics for three angiotensin IV analogs in rats. These characteristics include measures of metabolic stability, clearance mechanisms and rates, and kinetic parameters, including half life, volume of distribution, and area under the concentration/time curve. These studies indicate strong potential as pharmaceutical candidates for some of our angiotensin IV analogs; and a need for further chemical modification of others in order to overcome impractical pharmacokinetic characteristics. We additionally describe the development and validation of assays for quantification of these molecules in biological fluids.

TABLE OF CONTENTS

Page

LIST OF TABLES

LIST OF FIGURES

Dedication

This dissertation is dedicated to my family. Without your support and encouragement my success would not be possible.

CHAPTER ONE

INTRODUCTION, BACKGROUND AND SIGNIFICANCE

1.1. Cancer and Alzheimer's Disease – Two Pathologies, One Receptor

In 2005, malignant neoplasms and Alzheimer's disease were the second and seventh leading causes of death, respectively, in the United States (CDC 2008). At present, both of these diseases affect vast numbers of people every year, and treatment options are dismally limited. As of 2001, on average, the five year survival rate for individuals diagnosed with cancer was approximately 65%. Despite the extensive research efforts that have been focused on finding effective treatments for this disease, this is not much of an improvement over the five year survival rate of 51% seen in 1976 (American Cancer Society 2006). The prognosis for patients diagnosed with Alzheimer's is also poor. At present, there is no truly effective treatment for age-related dementia. Current medications administered to Alzheimer's patients provide moderate to no significant improvement in cognitive function, and, at best, only marginally slow the progress of the disease (Marum 2008).

The National Cancer Institute defines cancer as "diseases in which abnormal cells divide without control and are able to invade other tissues." Carcinogenesis is initiated when unrepaired DNA damage contributes to the dysregulation of the cell cycle resulting in uncontrolled proliferation. The occurrence of this proliferation marks the second stage in the process of carcinogenesis, termed promotion. The final step in the process, progression, occurs when the mass of cells resulting from uncontrolled proliferation display continued growth and invade other

tissues, developing into life-threatening disease. The metastatic process whereby malignant cells invade tissues, sometimes at sites distant from the site of original growth, is complex and requires an elaborate and impressive series of events within the metastatic cell. These include survival without cell-cell contact, secretion or recruitment of proteases for degradation of the extracellular matrix, migration, adhesion at a new site, proliferation in the new environment and neoangiogenesis or vascular mimicry to support continued growth. Any one of these events might represent a target for therapeutic intervention of the metastatic process.

The traditional approach has been to seek out methods of inhibiting uncontrolled cell proliferation and survival. Most chemotherapeutics available clinically work by this route. More recently, many investigators have focused on finding ways of preventing or reducing neoangiogenesis and vascular mimicry. In theory, this approach has a great deal of merit since neoangiogenesis is not a process normally occurring at a significant rate in a normal individual who is not pregnant, gaining significant weight, or healing from a serious injury. Therefore, targeting this process may yield therapies that exhibit minimal toxicity to normal tissues. However, in actuality, the situation is much more complicated. While depriving cancer cells of oxygen inhibits their ability to proliferate, the hypoxic environment also promotes Darwinian selection of cells that are more malignant and aggressive (Michieli 2009). This type of paradox seems to characterize the field of cancer research and demonstrates the complexity and confounding nature of the disease, which makes finding effective treatments so difficult. As yet, efforts have failed to produce highly effective treatments for many common types of cancer, including types of skin, lung, breast, colorectal, hematologic, and prostate cancers, to name just a few (CDC 2009).

Similarly, both traditional and new approaches to the development of treatments for Alzheimer's disease have failed to produce effective therapeutic options for those suffering from this or any other type of age-related dementia. However, unlike the situation within the field of cancer research, there is a lack consensus amongst Alzheimer's researchers on the most basic aspects of the physiology of the disease. There are two basic, competing schools of thought on the underlying processes governing the development of so-called "senile plaques" and neurofibrillary tangles, which characterize the disease. The "amyloid hypothesis" contends that senile plaques, which consist of extracellular deposits of the amyloid-β peptide, are causative and lead to neurofibrillary tangle formation, neurodegeneration and neuronal and synaptic loss (Allsop 2008). The opposing school of thought contends that amyloid plaques occur as a result of some other pathogenic factors and may even be a protective response by the neurons (Marum 2008).

Approaches to the treatment of Alzheimer's disease and other forms of dementia have primarily targeted certain neurotransmitter systems that have been shown to be altered in Alzheimer's patients. In particular, cholinesterase inhibitors are the most commonly prescribed therapy for patients with mild Alzheimer's disease. Clinical trials for the use of cholinesterase inhibitors show effects that can be described as modest at best (Hogan 2008). Memantine, an NMDA receptor antagonist, is used for the treatment of moderate to severe Alzheimer's disease with less clinical efficacy than that of the cholinesterase inhibitors (Marum 2008).

Initially, no apparent connection is evident that links these two largely dissimilar and apparently unrelated illnesses. However, our laboratory contends that these diseases share at least one physiological mechanism in common: the critical role of the Angiotensin IV-AT_4 receptor

system. Further, it is our contention that the AT_4 receptor represents an important and promising target for pharmacological intervention for both of these devastating diseases.

1.2. Angiotensin IV and the AT_4 Receptor

The AT_4 receptor is the most recently discovered member of a family of receptors that bind active members of the angiotensin family of molecules. Angiotensins are best known for their involvement in the renin-angiotensin system, which regulates blood pressure and fluid balance. All members of the angiotensin family are peptide hormones cleaved enzymatically from the precursor, angiotensinogen. Cleavage of the five c-terminal residues of angiotensinogen by the enzyme renin yields angiotensin I. Angiotensin II is a product of the action of the enzyme ACE on angiotensin I, which removes two additional residues at the c-terminus. Angiotensins III and IV are produced by the actions of aminopeptidases on angiotensins II and III, respectively. Angiotensin III consists of residues 2-8 of angiotensin II, and angiotensin IV consists of residues 2-7 of angiotensin III.

Angiotensins II, III and IV are the active members of the family and mediate their effects through the AT_1, AT_2 and AT_4 receptors. Angiotensins II and III bind, both, AT_1 and AT_2 receptors, and induce signaling that leads to vasoconstriction, electrolyte rebalancing, water retention, activation of the sympathetic nervous system and release of other hormones, including ADH and aldosterone (Paul 2006). Containing only six residues, angiotensin IV is the smallest member of the angiotensin family with known physiological activity (Table 1). Angiotensin IV is

a product of enzymatic removal of the n-terminal arginine of angiotensin III by alanyl aminopeptidase N (Wright 2008).

Angiotensin IV acts through binding of the AT_4 receptor and has a known role in a number of diverse physiological processes, primarily involving cognition and fluid balance. These include memory consolidation, learning, seizure protection, blood flow regulation, vascular repair and remodeling, and kidney function (Wright 1997, Tchekalarova 2005, Vinh 2008). Additional physiological process in which Angiotensin IV signaling has been shown to play a part include inflammation and wound healing, and the development of certain cancers (Esteban 2005, Ochedalska 2002, Pilar Carrera 2006).

From 1988 to the present, investigators have accumulated a substantial body of data in support of an important role for angiotensin IV in cognitive function. *In-vivo* administration of angiotensin IV has been shown to increase exploratory behavior and enhance acquisition in active and passive avoidance tests (Braszko 1988, Braszko 1991, Wright 1993). Angiotensin IV has also been shown to enhance long term potentiation, a putative measure of memory acquisition and storage (Wayner 2001), and induce hippocampal acetylcholine release (Lee 2001), *ex-vivo*. Likewise, angiotensin IV analogs have been shown to facilitate long term potentiation (Kramar 2001, Davis 2006), and to enhance spatial learning in the Barnes circular maze (Lee 2004). Angiotensin IV analogs have also been shown to reverse chemically and physically-induced cognitive deficits as tested in the Morris water maze task of spatial learning (Olson 2004, Pederson 1998, Wright 1999). These models of cognitive deficit involve disruption of the muscarinic cholinergic receptor system. Therefore the ability of angiotensin IV analogs to

overcome these deficits provides additional support to the idea that the cognitive effects of angiotensin IV involve the cholinergic system.

Involvement of the angiotensin IV-AT_4 receptor system in cancer is less well established. Still, three separate groups have unveiled apparent connections between angiotensin IV activity and carcinogenesis or tumor growth. In 2002, Ochedalska et al. demonstrated that both angiotensin II and angiotensin IV increased tyrosine kinase activity in pituitary tumors in rats (Ochedalska 2002). In 2004, Lawnicka et al. showed that exogenous administration of angiotensins II, III and IV inhibited the growth of human prostate cancer cells in-vitro (Lawnicka 2004). Finally, in 2006, Pilar Carrera et al. found that the activities angiotensin-metabolizing enzymes (insulin-regulated aminopeptidase (IRAP) and aminopeptidase N) were increased in rats with mammary tumors. This group concluded that the activity of these enzymes may be involved in the development of breast cancer through misregulation of the renin-angiotensin system (Pilar Carrera 2006).

Although a good deal of information has been obtained on the functions of the AT_4 receptor, the molecular identity of the AT_4 receptor and the specific mechanism of action of angiotensin IV-AT_4 signaling still remain largely unknown. However, a number of pieces to the overall puzzle have been ascertained. Several studies have attempted to determine the size of the AT_4 receptor with somewhat differing results. A study from our laboratory showed the receptor to consist of three subunits with estimated masses for the binding unit of 165 kDa in bovine adrenal gland, 150 kDa in bovine hippocampus and 125 kDa in bovine aorta (Zhang 1998). This study also showed the two additional subunits to be 50-60 kDa and 70-80 kDa. A study by another laboratory estimated the AT_4 receptor in bovine heart to have a transmembrane domain

of 153 kDa and an extracellular fragment of 143 kDa, with two small membrane associated fragments (Caron 2003).

It has been shown that activation of the AT_4 receptor leads to the influx of calcium in both neurons and kidney cells (Davis 2006, Dulin 1995, Handa 1999). Additionally, nitric oxide has been shown to be required for AT_4 activity (Coleman 1998, Vinh 2008, Toda 2007). The correlation of these data has led to the hypothesis that AT_4 receptor activation causes intracellular calcium mobilization and increased calreticulin expression that mediate the activation of eNOS, leading to the production of nitric oxide (Toda 2007). This hypothesis works well with the idea that the AT_4 receptor might be a serpentine G protein-linked receptor since G protein signaling could lead to the activation of phospholipase C and subsequent increases in calcium mobilization. Further, it is reasonable to assume that the AT_4 receptor might be a G protein-linked receptor based on the fact that both AT_1 and AT_2 are G protein-linked receptors and that most small peptide receptors are as well. However, several studies have shown that AT_4 binding is insensitive to guanine nucleotides (Hanesworth 1993, Wright 1997, Wright 2008), indicating that AT_4 is not G protein coupled.

Further evidence that AT_4 is not G protein coupled lies in the fact that angiotensin IV shares partial homology with angiostatin and the related plasminogen family member hepatocyte growth factor (HGF). HGF is the ligand for c-Met (Wright 2008), a membrane-spanning RTK (receptor tyrosine kinase). We have further investigated this homology and our data indicate that angiotensin IV analogs are able to induce or inhibit (in the case of our antagonists) HGF-dependant signaling (Yamamoto 2010). Additionally, angiotensin IV analogs are able to block the binding of HGF to c-Met with high affinity. These facts lead us to speculate that the AT_4

receptor and c-Met may in fact be the same receptor, or that angiotensin IV may mediate some of its effects through activation of c-Met.

1.3. The c-Met Receptor

C-Met was originally discovered as the product of the oncogene TPR-MET (Cooper 1984), and has in recent years been a popular target in cancer research. The c-Met receptor consists of a disulphide-linked heterodimer with 50 kDa extracellular α chain and a 145 kDa transmembrane β chain. Like AT_4, c-Met is expressed in a wide variety of tissues and cell types and across a wide range of species. Also like AT_4, c-Met is well known to be involved in vascular repair and remodeling, inflammation, wound healing and the development of certain cancers (Corso 2005, Singleton 2007). Additionally, c-Met has also been shown to be involved in regulation of blood pressure (Biswas 2005, Takiuchi 2004, Vistoropsky 2008) and improvement of cognitive function, both, after ischemic brain injury and in a model of Alzheimer's disease (Takeuchi 2008).

HGF/c-Met signaling is essential for embryogenesis and during development (Tulasne 2008), possessing the ability to direct stem cell proliferation and differentiation (Wright 2008). This is apparently the physiological reason for c-Met's activation of the so-called "invasive growth" program, which directs cells to proliferate and extravasate from their original location to new sites. Additionally, cell survival during this process is enabled in part by c-Met-directed protection from apoptosis (Migliore 2007). HGF/c-Met signaling also synergizes with the activity of vascular endothelial growth factor (VEGF) and its receptor to promote angiogenesis

and regulation of endothelial cells. These activities are the basis for c-Met involvement in tumorigenesis. Improperly regulated c-Met activity can occur by a number of mechanisms. c-Met can be over expressed (most common), mutated, excessively transactivated by other receptors, or over-activated by the establishment of misregulated HGF/c-Met autocrine loops.

The physiological functions described above also characterize c-Met activity in the brain where HGF/c-Met signaling is neurotrophic (Honda 1995) and protective (Zhang 2000, Tyndall 2007, Takeo 2007, Takeuchi 2008). As in other tissues, in the brain c-Met is involved in development, acting as a guidance factor during differentiation, motogenesis and neuritogenesis (Ebens 1996, Sun 2002, Tyndall 2007). HGF/c-Met signaling has also been shown to promote healing of neuronal injury (Trapp 2008), especially after ischemic brain injury (Takeo 2007).

1.4. Angiotensin IV Analogs

As mentioned briefly above, our laboratory has developed a library of synthetic AT_4 receptor ligands (angiotensin IV analogs) that show high affinity to both AT_4 and c-Met. This library consists of molecules containing modifications to the structure of angiotensin IV, including amino acid substitutions with naturally and non-naturally occurring amino acids and non-amino acid chemical moieties. Most of these substitutions have been made at the n- or c-terminus with the purpose of either serving to identify important structural features of the molecule, or to produce a molecule with better physicochemical and pharmacokinetic properties. The rational drug design approach has been employed in our laboratory to create molecules that

retain binding affinity and desired activity at the AT4/c-Met receptor, while exhibiting adequate metabolic stability for exogenous administration.

Within this library, one molecule in particular has demonstrated extremely promising activity as an anti-cancer agent. This molecule, an AT_4 receptor antagonist, has been named Norleual. The structure of Norleual is l-Norl-Tyr-Leu-(ψ)(CH_2NH_2)-His-Pro-Phe, which was constructed by changes to the first and third residues of angiotensin IV and the addition of a non-peptide bond after the third residue (Table 1). Norleual demonstrates a high level of potency and efficacy as an inhibitor of c-Met signaling and c-Met dependant cellular activity *in-vitro* (Yamamoto 2010). Further, Norleual inhibits metastasis in both breast and melanoma cancer models *in-vivo* (Yamamoto 2010).

A second molecule that has recently shown promising activity in *in-vitro* screening studies is another modified peptide exhibiting antagonist activity, which we named PNB-0405. PNB-0405 was constructed by the exchange of the valine in the first position of angiotensin IV to a norleucine with 'd' configuration, and the replacement of the three c-terminal residues with 6-amino-hexamide (Table 1). The resulting structure is d-Nle-Tyr-Ile-(6)amino-hexamide. PNB-0405 is expected to be more metabolically stable than Norleual due to the 'd' stereochemistry of the n-terminal amino acid and the addition of the 6-amino-hexamide to the c-terminus. Both structural features should help to protect the molecule from enzymatic degradation, while allowing it to retain affinity for the AT_4 receptor and ability to modulate c-Met signaling.

The third molecule is also a peptidomimetic but, unlike Norleual and PNB-0405, exhibits *agonist* activity. Labeled Dihexa, this molecule consists of a hexanoic acid in place of the first residue and a 6-amino-hexamide moiety in place of the 3 c-terminal residues (Table 1). The

resulting structure is hexanoic acid-Tyr-Ile-(6)amino-hexamide. Dihexa has exhibited promising activity as a potential cognition-enhancing agent in *ex-vivo* long-term potentiation studies and in behavioral studies using the Morris water maze task of spatial learning (unpublished data).

Table 1. Structure of Angiotensin IV Analogs.

Name	**Structure**
Angiotensin IV	Val-Tyr-Ile-His-Pro-Phe
Norleual	Nle-Tyr-Leu-(ψ)(CH_2NH_2)-His-Pro-Phe
PNB-0405	d-Nle-Tyr-Ile-(6)aminohexamide
Dihexa	Hexanoic-Tyr-Ile-(6)aminohexamide

1.5. Overview of Experimentation

The primary objective of the studies performed here was to determine the potential of these angiotensin IV analogs as therapeutic agents for the treatment of cancer or age-related dementia. For Norleual and PNB-0405, activity as anti-cancer agents has already been well established (Yamamoto 2010, unpublished data). Likewise, Dihexa has been shown to enhance cognitive activity in a number of paradigms. Therefore the focus of study for these molecules involves determining pharmacokinetic parameters as needed for optimization of dosing and preparation for eventual clinical studies. This dissertation is composed of four manuscripts, one

of which has been submitted for publication in a scientific journal. These manuscripts describe the basic pharmacokinetic and metabolic dispositions of these molecules.

CHAPTER TWO

HIGH-PERFORMANCE LIQUID CHROMATOGRAPHIC ANALYSIS OF NORLEUAL IN RATS

2.1. Introduction

The angiotensin family of molecules play important roles in many physiological processes, including body fluid homeostasis and vasoconstriction. Biologically active angiotensins are processed N-terminal fragments of the precursor protein, angiotensinogen. Angiotensin IV, a hexapeptide, is the smallest member of the angiotensin family of molecules with known physiological activity. Angiotensins primarily mediate their effects through the AT_1 and AT_2 receptors. Angiotensin IV, however, appears to act through a separate signaling pathway not involving AT_1 or AT_2. Additionally, its effects are dissimilar and sometimes opposite to those of other angiotensin family members (Hamilton 2001, Wayner 2001).

Investigation of angiotensin IV signaling, structure and physiological activity has prompted our laboratory to develop a library of angiotensin IV analogs. Within this library, several molecules have emerged that exhibit especially interesting physiological activity supporting a role for angiotensin IV that is quite different from that of other angiotensin family members. We have recently published data indicating that the angiotensin IV analog, Norleual (Nle-Tyr-Leu-ψ[CH_2-NH_2]-His-Pro-Phe), acts as a potent inhibitor of the c-Met receptor tyrosine kinase (Yamamoto 2010).

The c-Met receptor tyrosine kinase, often referred to simply as Met, is activated by binding of its ligand, hepatocyte growth factor (HGF). Met activation is directly or indirectly involved in pro-metastatic cellular processes, including proliferation, migration, epithelial-mesenchymal transition, and scattering. These activities have made Met a popular target for cancer therapy research in recent years. Further, HGF-Met signaling is pro-angiogenic and a number of Met and HGF antagonists inhibit angiogenesis (Migliore 2008, You 2008, Toschi 2008). This is also the case for our putative HGF/Met antagonists.

A putative HGF/Met-antagonist, Norleual (Table 2.1), shows promise as an anti-angiogenic/anti-cancer therapeutic candidate *in-vitro* and also in mouse models (Yamamoto 2010). An initial required step in the development of Norleual as a clinical candidate is a complete pharmacokinetic characterization. In order to complete a successful pharmacokinetic study, it is first necessary to establish and validate an analytical method by which Norleual concentrations in blood can be determined consistently and accurately. Because, to our knowledge, there are no published methods for the analysis of angiotensin IV analogs, our first goal was to develop an analytical method. Thus, this study reports the validation of a simple, selective, reversed-phase HPLC/mass spectrometry analysis method for the detection and quantification of Norleual in blood.

Table 2.1 Structure of Angiotensin IV, Norleual and the Internal Standard

Name	**Structure**
Angiotensin IV	Val-Tyr-Ile-His-Pro-Phe
Norleual	Nle-Tyr-Leu-(ψ)(CH_2NH_2)-His-Pro-Phe
PNB-0719 (Internal Standard)	Nle-Tyr-Ile-His-Pro-Phe

2.2. Methods

2.2.1. Chemicals and Reagents

HPLC grade methanol, acetonitrile and water, and reagent grade heptafluorobutyric acid were purchased from Sigma (St. Louis, MO, USA). Norleual was synthesized by Syngene (Bangalore, India) according to the protocol developed in our laboratory (unpublished) and purified in our laboratory by reverse phase HPLC.

2.2.2. Sample Preparation

Fresh rat blood was obtained prior to each experiment via indwelling jugular vein catheters from adult male Sprague-Dawley rats.

Norleual solutions were prepared in HPLC grade water at the concentrations specified. Stock Norleual was kept in powder form and stored at -20ºC. Quality control (QC) samples were prepared by spiking fresh rat blood on ice with an appropriate dilution of Norleual in water for the final concentration of Norleual specified, keeping a 10:1 ratio of blood to Norleual solution. The compound, PNB-0719, a molecule very similar in structure (Table 2.1 shows structure) and properties to Norleual, was used as an internal standard and was prepared and added to blood samples in the same way.

The proteins present in the blood samples were immediately (no more than 1 minute after spiking) precipitated using 3 volumes of ice-cold acetonitrile (ACN), vortexed for approximately

10 seconds, and centrifuged at 5000 RPM for 5 minutes. The supernatants were transferred to new tubes and stored until use if necessary at 4ºC. The samples were then evaporated to dryness in a Savant SpeedVac® concentrator. The residue was reconstituted in 225µl of 35% methanol and vortexed briefly, then transferred to autosampler vials.

2.2.3. Chromatographic System and Conditions

The HPLC/MS system used was from Shimadzu (Kyoto, Japan), consisting of a CBM-20A communications bus module, LC-20AD pumps, SIL-20AC auto sampler, SPD-M20A diode array detector and LCMS-2010EV mass spectrometer. Data collection and integration were achieved using Shimadzu LCMS solution software.

The analytical column used for separation was an Econosphere C18 (100mm x 2.1mm) from Grace Davison Discovery Science (Deerfield, IL, USA). The mobile phase consisted of ACN and HPLC water with 0.1% heptafluorobutyric acid. Separation was carried out using a gradient method, starting at 30% ACN and increasing to 60% ACN over 7 minutes, at ambient temperature and a flow rate of 0.3 mL/min. For MS analysis, a positive ion mode (scan) was used to monitor the m/z of Norleual at 388 and the m/z of PNB-0719 (internal standard) at 395. Samples were introduced using an autosampler with an injection volume of 100µl.

2.2.4. Animals and Surgical Procedures

Male Sprague-Dawley rats (250+ g) were obtained from Harlan Laboratories (CA, USA) and allowed food (Harlan Teklad rodent diet) and water *ad libitum* in our animal facility. Approval for animal experimentation was obtained from the Washington State University Animal Care and Use Committee. Rats were housed in an AAALAC accredited facility in temperature-controlled rooms on a 12 hour light/dark cycle. The right jugular veins of the rats were catheterized with sterile polyurethane Hydrocoat™ catheters (Access Technologies, Skokie, IL, USA) under ketamine (Fort Dodge Animal Health, Fort Dodge, IA, USA) and isoflurane (Vet One™, MWI, Meridian, ID, USA) anesthesia. The catheters were exteriorized through the dorsal skin between the scapulae. The catheters were flushed with heparinized saline before and after blood sample collection and filled with heparin-glycerol locking solution (6 mL glycerol, 3 mL saline, 0.5 mL gentamycin (100mg/mL), 0.5 mL heparin (10,000 u/mL)) when not sampled for more than 8 hours.

2.2.5. Method Validation

2.2.5.1. Recovery

Recovery of Norleual and PNB-0719 from biological fluids was assessed (n = 3) at 10ug/mL by spiking blood samples with Norleual or PNB-0719. Samples were then prepared as described above (section 2.2.2). The LCMS response for these samples was compared to that of freshly prepared samples of Norleual and PNB-0719 in water.

2.2.5.2. Selectivity

Selectivity was evaluated by peak purity analysis using chromatograms from the same samples used for the precision and accuracy experiment.

2.2.5.3. Precision and Accuracy

The precision and accuracy of standard Norleual determination was established by preparing three sets of standards consisting of six concentrations of Norleual in blood (0.5, 1, 5, 10, 50 and 100 μg/mL). Each of the three sets of QC samples was prepared separately from scratch (starting from stock Norleual powder). Samples were prepared by spiking blood aliquots with Norleual and processing as described above (section 2.2). The between-run precision and accuracy of the assays were estimated using the peak area ratios from each set of samples.

2.2.5.4. Lower Limit of Quantification

The lower limit of quantification (LLOQ) was established as the lowest concentration of Norleual that could be quantified with an average bias of less than 20%.

2.2.5.5. Stability Studies

To determine the stability of Norleual in blood, Norleual was spiked in parallel into blood and 30% ethanol (n=3 per time point) and the samples placed in an incubator at 37ºC. At 0, 20, 40, and 60 minutes, a set of samples was removed from the incubator and prepared for high-performance liquid chromatography as described above. Stability half-lives were determined assuming a normal single phase exponential decay.

The stability of Norleual in blood samples, which were extracted with ACN and stored in ACN at 4ºC, was determined over a 3.5 hour time period. Stability of Norleual in blood samples extracted by precipitation with ACN and stored in the autosampler rack (15ºC) was monitored for 60 minutes. For these studies, stability was established by comparing the response of Norleual in stored samples with those of freshly prepared samples at the same concentration.

2.3. Results and Discussion

2.3.1. Selectivity and Chromatography

In order to determine the most optimal chromatographic method for separation and resolution of Norleual and the internal standard, optimization of the mobile phase composition and gradient was performed. The addition of 0.1% (v/v) heptafluorobutyric acid as an ion-pairing agent enhanced separation between Norleual and the internal standard, as compared to acetic acid, trifluoroacetic acid or no acid. Norleual exhibited a later elution time with heptafluorobutyric acid-containing mobile phase, thus providing sufficient separation of Norleual and the internal standard, which eluted together in the absence of heptafluorobutyric acid. The efficiency of the acetonitrile (ACN) gradient was evaluated with regard to the rate of change (3.3% per minute to 10% per minute) as well as initial conditions (0% ACN up to 50% ACN). These studies established an optimal organic gradient of 30 to 60% over 7 minutes with a flow rate of 0.3mL/min. This mobile phase composition was employed throughout the study because it provided optimal separation and peak shape with minimal run time.

Excellent separation and baseline resolution of Norleual and the internal standard in blood was successfully achieved (Figure 2.1). Norleual eluted at 4.4 minutes while the internal standard eluted at 5.2 minutes. No interfering peaks co-eluted with the analyte or internal standard (Figure 2.1). Peak purity analysis performed by LCSolution® software revealed a peak purity index for both Norleual and the internal standard of 0.9995.

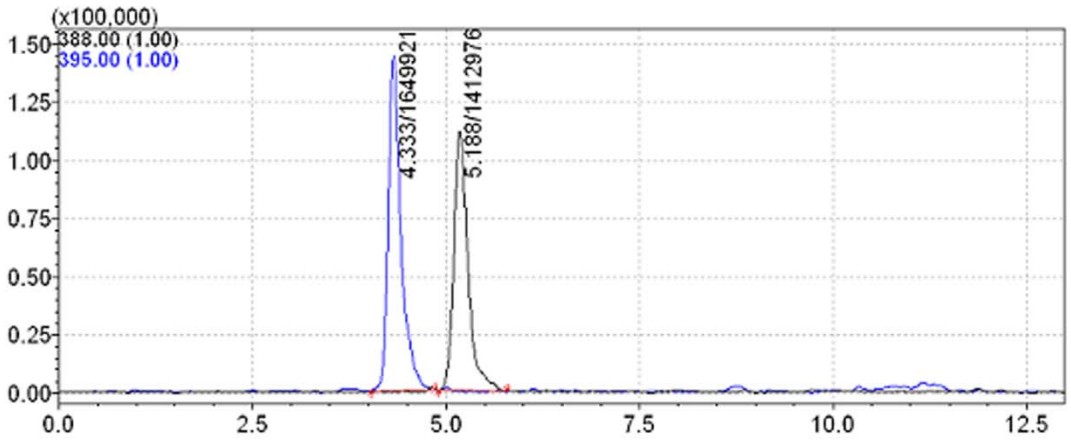

Figure 2.1 Representative chromatogram of Norleual (m/z 388.00) and internal standard (m/z 395.00) recovered from rat blood in which the concentration of Norleual was 5ug/mL. The chromatographic conditions consisted of an Econosphere C18 (100mm x 2.1mm) column and mobile phase consisting of acetonitrile and water with 0.1% heptafluorobutyric acid. Separation was achieved using a gradient starting at 30% acetonitrile and increasing to 60% acetonitrile over 7 minutes at ambient temperature and a flow rate of 0.3mL/min.

2.3.2. Recovery

The recovery of Norleual and the internal standard, PNB-0719, extracted from blood by acetonitrile protein precipitation, was determined in three replicate samples containing Norleual (10µg/mL) or PNB-0719 (10µg/mL) spiked into blood. The mean extraction efficiency of this method for Norleual was 92.5% and 75.6% for PNB-0719 (Table 2.2).

Table 2.2 Recovery of Norleual and PNB-0719 from blood compared to water controls (n = 3).

	Recovery (%) (mean ± SD)
Norleual	92.5 ± 9.2
PNB-0719	75.6 ± 4.8

2.3.3. Precision and Accuracy

Table 2.3 shows within- and between-run precision and accuracy for the determination of Norleual concentrations in blood. The within- and between-run bias for the determination of Norleual concentrations in blood was less than 15%, except at the LLOQ (0.5µg/mL). The maximum deviation of estimated values from actual values was 12.34% within-run, and 13.1% between-runs, excluding the LLOQ. Precision was determined based on relative standard deviation (R.S.D.) of the calculated concentrations. R.S.D. values were below 15% for within-run calculations. R.S.D. values for between-run calculations were below 20%. These data indicate that the method is accurate and reproducible.

Table 2.3 Within- and between-run precision and accuracy of the assay for Norleual in blood (n = 3, mean ± SD)

Concentration (µg/mL)	**Precision (average ± SD)**		**Accuracy**			
	Within-run	**Between-run**	**Within-run**		**Between-run**	
	(µg/mL)	**(µg/mL)**	**%**	**Bias (%)**	**%**	**Bias (%)**
100	100.04 ± 0.07	96.97 ± 12.13	100.04	0.04	96.97	-3.03
50	49.86 ± 0.23	49.32 ± 2.65	99.72	-0.28	98.64	-1.36
10	10.64 ± 0.89	11.31 ± 2.06	106.38	6.38	113.10	13.10
5	4.38 ± 0.65	4.64 ± 0.22	87.66	-12.34	92.81	-7.19
1	1.00 ± 0.09	1.01 ± 0.15	100.42	0.42	101.37	1.37
0.5	0.59 ± 0.05	0.57 ± 0.08	117.15	17.15	113.42	13.42

2.3.4. Curve-Fit and LLOQ

The relationship between concentration and response was fit to a Boltzmann sigmoidal equation with an r^2 value of ≥ 0.999. The lower limit of quantification (LLOQ) for the determination of Norleual concentrations in blood was 0.5µg/mL. This is the lowest concentration that could be quantified with an average bias of less than 20%.

2.3.5. Stability Studies

The stability of Norleual in acetonitrile was assessed using blood samples spiked with Norleual and then precipitated with three volumes ice-cold acetonitrile (n = 3) as per the method protocol. The acetonitrile-precipitated samples were then either held at 4ºC for 3.5 hours or immediately prepared for high-performance liquid chromatography. There was an 8.65 ± 2.89% reduction in the response for the samples held for 3.5 hours in acetonitrile at 4ºC.

The stability of Norleual extracted from blood samples and stored in the autosampler at 15ºC for 1 hour was also assessed. There was no reduction in the responses for these samples, indicating Norleual extracted from blood and reconstituted in 35% methanol is stable at 15ºC for at least an hour. In fact, there was an average 14.62% increase in response after 1 hour. This may suggest that it may be advantageous to allow samples time to equilibrate with the temperature of the autosampler before commencing analysis. A lack of degradation of the Norleual samples stored in the autosampler at 15ºC was evident even after several days.

The stability of Norleual in blood was assessed (n = 3) by comparing samples of Norleual spiked in blood to samples of Norleual spiked in 30% ethanol (Figure 2.2). There was a 93.86% reduction in response between zero minute blood samples and 20 minute blood samples, indicating significant loss of Norleual in blood over the first 20 minutes. Reduction in response between 20 and 40 minutes, and between 40 and 60 minutes was 4.28% (of initial response) and 0%, respectively. These data indicate that Norleual is unstable in the blood at 37ºC. The calculated stability $t_{1/2}$ value based on a single phase exponential decay was 4.56 minutes (r^2 = 1.00).

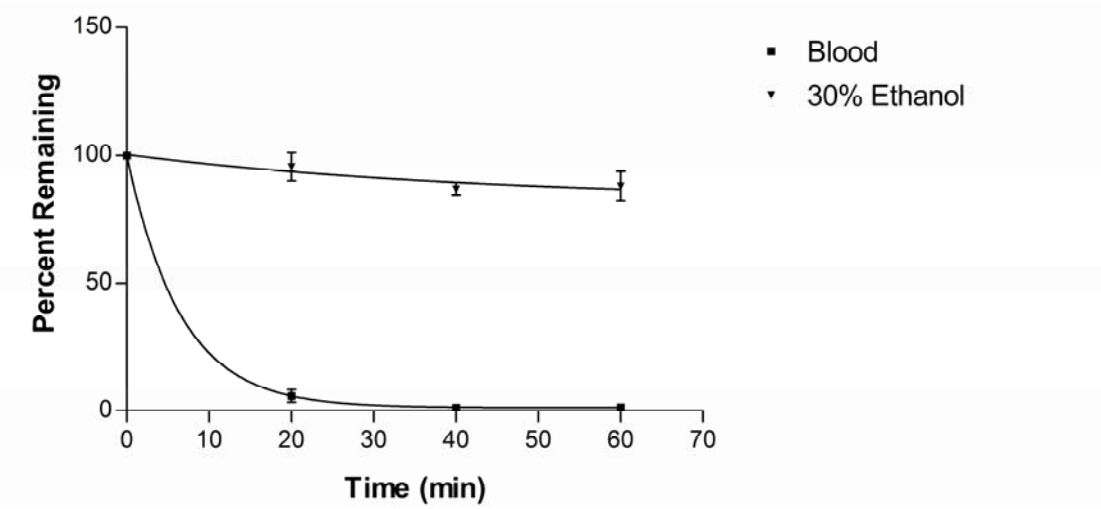

Figure 2.2 Stability of Norleual in rat blood stored at 37ºC as compared to Norleual stored in 30% ethanol (v/v) at 37ºC (n = 3). Percent recovery over time (mean ± SD). Closed triangles represent values for ethanol Norleual samples. Closed squares represent values for blood Norleual samples.

2.4. Conclusion

In summary, a simple, reproducible, accurate, and sensitive HPLC-MS assay was developed for the detection and quantification of Norleual suitable for analysis in rat blood. Further studies are being conducted in our laboratory to characterize the disposition of Norleual. There is currently no other assay for detection of Norleual in blood published in the literature. This method is practical and efficient and provides a validated means of determining Norleual concentrations in the blood for pre-clinical applications.

CHAPTER THREE

PHARMACOKINETICS AND METABOLISM OF NORLEUAL IN RATS

3.1. Introduction

Synthetic analogs of the hexapeptide hormone angiotensin IV have been under investigation for their diverse and potent effects on cellular mechanisms related to cancer and other disorders, including angiogenesis, uncontrolled growth, and escape from apoptosis. Our laboratory has synthesized large number and variety of angiotensin IV analogs, some of which have shown compelling activity as anti-cancer agents. The angiotensin IV analog, Norleual (l-Norl-Tyr-Leu-(ψ)(CH_2NH_2)-His-Pro-Phe), has recently been shown to act as a potent inhibitor of the HGF/c-Met signaling cascade and to act as an anti-cancer agent *in-vitro* and *in-vivo* (Yamamoto 2010).

The c-Met receptor is a tyrosine kinase that is activated by binding of its cognate ligand HGF (hepatocyte growth factor) to initiate signaling cascades that lead to cytoskeletal reorganization and promote survival and proliferation. The c-Met receptor is expressed in almost all tissues and plays critical roles during fetal development and in the processes of wound healing and tissue repair (Knudsen 2008). Dysregulated c-Met activity has been shown to be critical in a number of cancers including gastric and lung cancers (Benvenuti 2007) and aberrant c-Met expression is found in a variety of cancers including thyroid, renal cell, prostate, ovarian and colorectal cancers (Migliore 2007).

A number of approaches have been taken to develop therapeutics that target HGF/c-Met signaling for the treatment of cancer. These include, most notably, small-molecule tyrosine kinase inhibitors and monoclonal antibodies targeting HGF or c-Met (Eder 2009). However, an effective and specific inhibitor of HGF/c-Met signaling for cancer therapy remains elusive. Our putative HGF/c-Met signaling antagonist, Norleual, has been shown to compete with high affinity for binding to the c-Met receptor, to inhibit c-Met activated signaling cascades, to inhibit HGF-dependant cellular proliferation and scattering, to inhibit angiogenesis *ex-vivo*, and to inhibit metastasis *in-vivo* (Yamamoto 2010).

In order to further develop our understanding of Norleual and determine its candidacy as a potential pharmaceutical agent, it is necessary to establish an understanding of its pharmacokinetics. Our laboratory has developed a selective, accurate and reproducible assay using high performance liquid chromatography-mass spectrometry for quantification of Norleual concentrations in rat blood (unpublished data). Here we describe the pharmacokinetic disposition of Norleual in rats. The validated method was used to analyze blood samples following intravenous administration of Norleual in rats via jugular vein catheters. The binding of Norleual to albumin and the stability of Norleual in the presence of rat liver microsomes were also investigated *in-vitro* in order to further examine Norleual kinetics and metabolism.

3.2. Methods

3.2.1. Chemicals and Reagents

HPLC grade ethanol, methanol, acetonitrile and water, reagent grade trifluoroacetic acid, sodium bicarbonate and heparin sodium salt were purchased from Sigma (St. Louis, MO, USA). Phosphate buffered saline (PBS) was purchased from BioRad (Hercules, CA, USA). Tris was purchased from Fisher (Fair Lawn, NJ, USA).

3.2.2. Preparation of Standards

Norleual stock solutions were prepared by dissolving lyophilized Norleual powder in HPLC grade water at 1 mg/mL. This solution was used to make lower concentration samples by serial dilution in HPLC grade water.

3.2.3. Equilibrium Dialysis

The Rapid Equilibrium Dialysis (RED) kit was purchased from Thermo Scientific (Waltham, MA, USA). The kit protocol was followed. Briefly, the kit base plate was rinsed in 20% ethanol for 10 minutes, then rinsed twice in distilled water and allowed to dry. RED inserts were placed in the base plate. Bovine serum albumin (BSA) (Sigma, St. Louis, MO, USA) was prepared in lactated Ringer's solution at 4 g/dL. 63µL of 1mg/mL Norleual was added to each of

three aliquots of 567µL lactated Ringer's (used for controls) and three aliquots of 567 µL BSA solution. 200 µL from each sample was transferred into each sample chamber, and 350 µL PBS was transferred into each of the corresponding buffer chambers. The plate was covered with sealing tape and incubated at room temperature on a shaker table over night. 50 µL from each chamber was transferred into clean microcentrifuge tubes. 50 µL PBS was added to the BSA/lactated Ringer's samples and 50 µL BSA or pure lactated Ringer's was added to corresponding PBS samples. 300 µL ice-cold acetonitrile was added to each sample and the samples were held on ice for 30 minutes. The samples were centrifuged at 5000 RPM for 5 minutes and supernatants were transferred into clean tubes. The samples were then evaporated to dryness in a Savant SpeedVac® concentrator and reconstituted in 225 µL HPLC grade water and analyzed by high performance liquid chromatography according to the method described in 3.2.8.

3.2.4. Microsomal Study

Male rat liver microsomes were obtained from Celsis (Baltimore, MD, USA). The protocol from Celsis for microsome-drug incubation was followed with minor adaptations. An NADPH regenerating system (NRS) was prepared as follows: 1.7 mg/mL NADP, 7.8 mg/mL glucose-6-phosphate and 6 units/mL glucose-6-phosphate dehydrogenase were added to 10 mL 2% sodium bicarbonate. The NRS was used immediately. 500 µM solutions of Norleual, piroxicam, (±)-verapamil and 7-ethoxycoumarin (low, moderate and highly metabolized controls, respectively) were prepared in acetonitrile. Microsomes were suspended in 0.1M Tris

buffer (pH 7.38) at 0.5 mg/mL. 100 µL microsomes was added to pre-chilled microcentrifuge tubes on ice. To each sample, 640 µL 0.1M Tris buffer and 10 µL 500 µM test compound were added. The samples and NRS were placed in a water bath at 37ºC for 5 minutes. The samples were removed from the water bath and 250 µL NRS was added to each. The samples were placed into a rotisserie hybridization oven at 37ºC with rotation at high speed for the appropriate incubation time (10, 20, 30 40 or 60 minutes). 500 µL from each sample was transferred to each of two tubes containing 500 µL ice-cold acetonitrile with internal standard per incubation sample. Standard curve samples were prepared in incubation buffer and 500 µL added to 500 µL ice-cold acetonitrile with internal standard. All samples were then analyzed by high performance liquid chromatography/mass spectrometry. Drug concentrations were determined and loss of parent relative to negative control samples containing no microsomes was calculated. Clearance was determined by nonlinear regression analysis for k_e and $t_{1/2}$ and the equation $Cl_{int} = k_e$ Vd. For *in vitro-in vivo* correlation, Cl_{int} per kg body weight was calculated using the following measurements for Sprague-Dawley rats: 44.8 mg of protein per g of liver, 40 g of liver per kg of body weight (obtained from Naritomi, 2001).

3.2.5. Animals and Surgical Procedures

Male Sprague-Dawley rats (250+ g) were obtained from Harlan Laboratories (CA, USA) and allowed food (Harlan Teklad rodent diet) and water *ad libitum* in our animal facility. Rats were housed in temperature-controlled rooms with a 12 hour light/dark cycle. The right jugular veins of the rats were catheterized with sterile polyurethane Hydrocoat™ catheters (Access

Technologies, Skokie, IL, USA) under ketamine (Fort Dodge Animal Health, Fort Dodge, IA, USA) and isoflurane (Vet One™, MWI, Meridian, ID, USA) anesthesia. The catheters were exteriorized through the dorsal skin. The catheters were flushed with heparinized saline before and after blood sample collection and filled with heparin-glycerol locking solution (6 mL glycerol, 3 mL saline, 0.5 mL gentamycin (100mg/mL), 0.5 mL heparin (10,000 u/mL)) when not used for more than 8 hours. The animals were allowed to recover from surgery for several days before use in any experiment, and were fasted over night prior to the pharmacokinetic experiment.

3.2.6. Pharmacokinetic Study

Male Sprague Dawley rats were catheterized as described in the Animals and Surgical Procedures section. The animals were placed in metabolic cages prior to the start of the study and time zero blood samples were collected. The animals were then dosed intravenously via the jugular vein catheters, with Norleual (89 mg/kg) suspended in water. After dosing, blood samples were collected as follows (times and blood volumes collected are listed in chronological order):

Dosage Route	**Time (minutes)**	**Blood Volume Collected (µl)**
Intravenous	0, 3.5, 9, 15, 25, 40, 60, 90	150, 150, 200, 200, 300, 400, 500, 600

After each blood sample was taken, the catheter was flushed with heparinized saline or heparinized Ringer's solution and a volume of heparinized saline or Ringer's equal to the volume of blood taken was injected (to maintain total blood volume).

3.2.7. Blood Sample Preparation

The samples were collected into polypropylene microcentrifuge tubes containing a volume of internal standard (PNB-0719, 100 ug/mL) equal to 0.1 times the sample blood volume collected, and cooled on ice for 30 seconds. A volume of ice-cold acetonitrile equal to three times the sample blood volume was then added and the sample vortexed vigorously for 30 seconds. The samples were then held on ice until the end of the experiment and stored at -20ºC afterward until further processing. Serial dilutions of Norleual in water were prepared from the stock used to dose the animals to be used for preparation of a standard curve. 20 µL of each serial dilution was then added to 180 µL of heparinized blood on ice for final concentrations of 0.01 µg/mL, 0.05 µg/mL, 0.1 µg/mL, 1 µg/mL, 10 µg/mL, 50 µg/mL and 100 µg/mL. 0.1 volume (20 µL) of PNB-0719 was then added to each sample as an internal standard. Three volumes of ice-cold acetonitrile (600 µL) was added and the samples vortexed vigorously. The standard curve blood samples were then stored at -20ºC and further processed alongside the pharmacokinetic study samples. All samples were centrifuged at 5000 RPM for 5 minutes and a volume of supernatant equal to the volume of acetonitrile added is transferred to clean tubes. The samples were then evaporated to dryness in a Savant SpeedVac® concentrator. The residue was reconstituted in 225 µl water and vortexed briefly. The samples were then transferred to HPLC autosampler vials and 100 µl is injected into the HPLC system a total of 2 times (2 HPLC/MS analyses) for each sample.

3.2.8. Chromatographic System and Conditions

The HPLC/MS system used was from Shimadzu (Kyoto, Japan), consisting of a CBM-20A communications bus module, LC-20AD pumps, SIL-20AC auto sampler, SPD-M20A diode array detector and LCMS-2010EV mass spectrometer. Data collection and integration were achieved using Shimadzu LCMSsolution software. The analytical column used was an Econosphere C18 (100mm x 2.1mm) from Grace Davison Discovery Science (Deerfield, IL, USA). The mobile phase consisted of HPLC grade acetonitrile and water with 0.1% heptafluorobutyric acid. Separation was carried out using a non-isocratic method at ambient temperature and a flow rate of 0.3 mL/min. For MS analysis, a positive ion mode (Scan) was used to monitor the m/z of Norleual at 388 and the m/z of PNB-0719 (used for internal standard) at 395. For the microsomal study, the m/z of (±)-verapamil was 455, the m/z of piroxicam was 332, and the m/z of 7-ethoxycoumarin was 191.

3.2.9. Pharmacokinetic Analysis

Pharmacokinetic analysis was performed using data from individual rats. The mean and standard deviation (SD) were calculated for the group. Noncompartmental pharmacokinetic parameters were calculated from blood drug concentration-time profiles by use of WinNonlin® software (Pharsight, Mountain View, CA, USA). The following relevant parameters were determined where possible: area under the concentration-time curve from time zero to the last time point ($AUC_{0\text{-}last}$) or extrapolated to infinity ($AUC_{0\text{-}\infty}$), C_{max} concentration in plasma

extrapolated to time zero (C_0), terminal elimination half-life ($t_{1/2}$), volume of distribution (Vd), and clearance (CL).

3.3. Results and Interpretation

3.3.1. Modeling of Physicochemical Properties and Plasma Protein Binding

In order to estimate basic physicochemical properties of Norleual, the molecule was modeled using ADMET Predictor® software (Simulations Plus Inc., Lancaster, CA, USA). Table 3.1 shows the resulting values for parameters of interest.

Table 3.1 Predicted Physicochemical Properties of Norleual

Physicochemical Property	**Predicted Value**
logP	0.68
P_{eff}	0.28
P_{avg}	0.08
Pr_{Unbnd}	13.32

The octanol-water partition coefficient, or logP value, represents the log transformation of the octanol:water partition ratio and is a measure of hydrophilicity. A predicted logP value of 0.68 for Norleual indicates that, in a mixture of octanol and water, for every 1 mol of Norleual that partitions into water, 4.79 mol Norleual partition into octanol. This indicates that Norleual is somewhat hydrophobic. The P_{eff} and P_{avg} values are predictors of intestinal permeability, and therefore, oral bioavailability. The P_{eff} value represents the predicted effective human jejunal permeability and P_{avg} represents the predicted average intestinal permeability along the entire human intestinal tract. The predicted P_{eff} value for Norleual of 0.28 and the predicted P_{avg} value for Norleual of 0.08 are lower than the predicted values of other orally administered drugs in use

in the clinic that were modeled for comparison, including caffeine, enalapril, piroxicam and carbamazepine. This result suggests that Norleual may not be a candidate for oral administration. However, this is modeling data only and should not be considered as an equivalent substitute for experimental determination of these properties.

The parameter Pr_{Unbnd} represents the percent of Norleual not bound to plasma proteins in circulation. Norleual is predicted to be only 13.32% unbound to plasma proteins. However, experimental data in our laboratory indicated that the percent Norleual unbound to albumin was 92.23 ± 10.42 %. This result was obtained by equilibrium dialysis experiments performed with a solution of bovine serum albumin (BSA) at normal physiological concentration. Albumin is the primary protein component in blood responsible for drug binding. The short half-life of Norleual in blood, which we have previously reported (McCoy 2010 submitted) prohibits the use blood or plasma for equilibrium dialysis experiments for determination of Norleual plasma protein binding. We therefore performed plasma protein binding experiments using a solution of BSA. These data suggest that in the blood Norleual may be highly bound to plasma proteins other than albumin, such as alpha-1-acid-glycoprotein.

3.3.2. Intrinsic Clearance of Norleual in Male Rat Liver Microsomes

Phase I metabolism of Norleual was investigated by pooled male rat liver microsomes. Under the experimental conditions, Norleual concentrations diminished at a rate that was consistent with an intrinsic clearance (Cl_{int}) of 67.66 ± 5.65 μL/min/mg, and a half life of 20.49 minutes. The percent Norleual remaining vs. time curve was fit to a one-phase exponential decay

curve with an R^2 value of 0.9926 (Figure 3.1). These data indicate that Norleual is susceptible to metabolism by phase I enzymes. The stability of piroxicam, (±)-verapamil and 7-ethoxycoumarin were also tested as high, moderate and low metabolized controls, respectively, with mean values that were within the ranges of those posted in the literature (Table 3.2) (Di 2003, Shou 2005, Lu 2006, Behera 2008). Percent remaining vs. time curves for the reference compounds are shown in Figure 3.2.

Table 3.2. Intrinsic clearance values for Norleual and reference compounds (mean ± SD, n = 3 per time point per compound).

Test Compound	**Intrinsic Clearance (µL/min/mg)**
Norleual	67.66 ± 5.65
7-Ethoxycoumarin	136.7 ± 10.17
(±)-Verapamil	112.52 ± 504.80
Piroxicam	60.22 ± 77.58

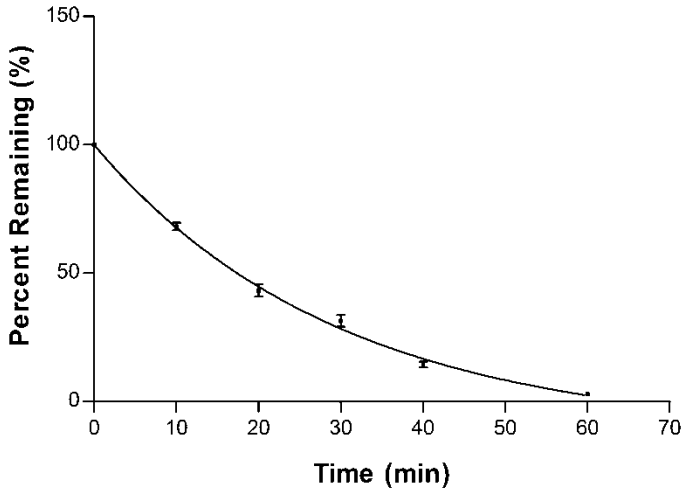

Figure 3.1 Metabolic stability profile for Norleual incubated with male rat liver microsomes (n = 3). Percent remaining over time (mean ± SE).

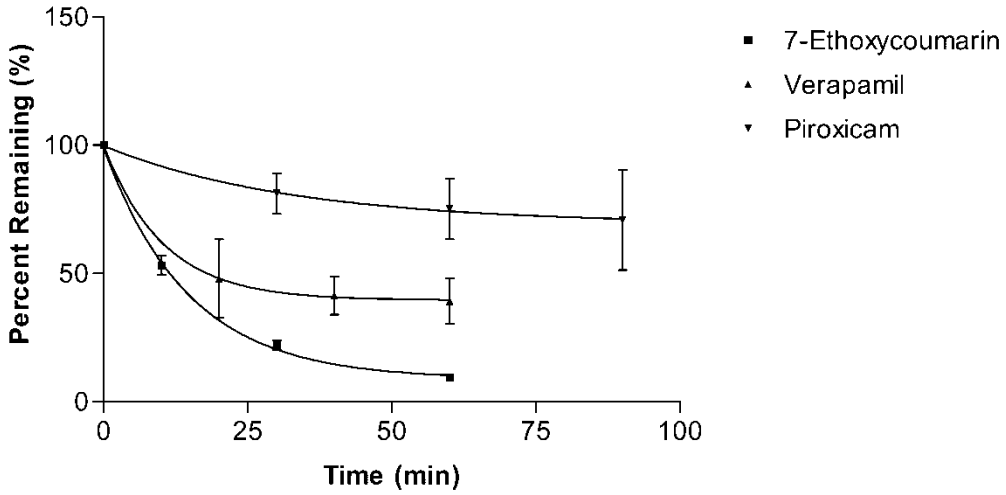

Figure 3.2. Metabolic stability profile for 7-Ethoxycoumarin, (±)-Verapamil and Piroxicam incubated with male rat liver microsomes (n = 3). Percent remaining over time (mean ± SE).

3.3.3. *In-vivo* Pharmacokinetics Studies

Norleual was administered intravenously to adult male rats via jugular vein catheters. The blood concentration versus time profile (Figure 3.3) was biphasic with a short distribution phase lasting from 0 to 15 minutes followed by a pure elimination phase in which blood concentrations were extremely low, but relatively stable. Blood concentrations at 25 to 90 minutes were below the validated limit of quantification for the assay (0.5 μg/mL). After 90 minutes, blood levels were below the limit of detection.

Norleual pharmacokinetic parameters were estimated using non-compartmental analysis with WinNonlin® software and are summarized in Table 3.3. In agreement with the relatively high rate of metabolism exhibited by Norlueal in the metabolic stability study, Norleual exhibited a relatively short elimination half life ($t_{1/2}$) of 28.0 ± 10.8 minutes. The volume of distribution (Vd) was 1.8 ± 0.4 L/kg, indicating Norleual resides predominantly in the central blood compartment and is not highly distributed into the tissues. Total body clearance of Norleual was estimated to be 0.057 ± 0.013 L/min/kg.

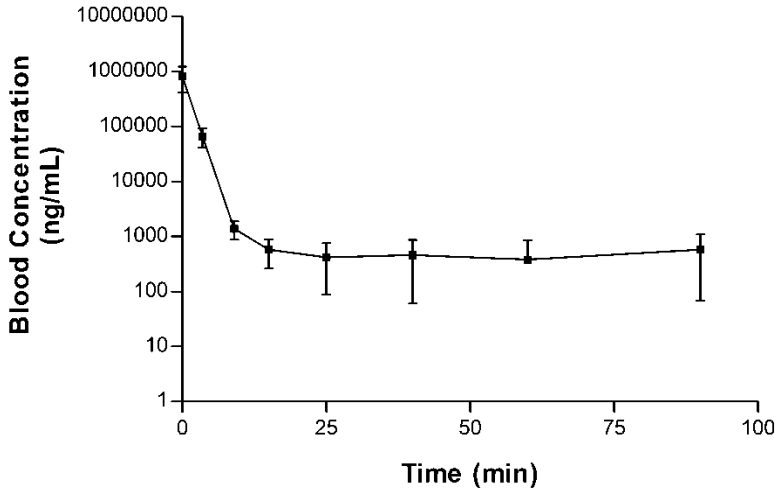

Figure 3.3 Blood concentrations of Norleual after intravenous bolus dose administration (89 mg/kg) in male Sprague-Dawley rats (n = 4, mean ± SD).

Table 3.3 WinNonlin® estimated pharmacokinetic paramters for Norleual after intravenous administration to adult male Sprague-Dawley rats (n = 4).

Pharmacokinetic Parameter	**Mean**	±	**SEM**
$AUC_{0-\infty}$ (min.ng/mL)	1863051.1	±	530304.7
Vd (L/kg)	1.8	±	0.4
C_p^0 (ng/mL)	827803.2	±	247039.1
$t_{1/2}$ (min)	28.0	±	10.8
KE (min^{-1})	0.044	±	0.021
CL (L/min/kg)	0.057	±	0.013

3.3.4. *In vitro-in vivo* Correlation

In vitro-in vivo correlation of data from the microsome and pharmacokinetic studies suggest that the primary route of clearance for Norleual that is not degraded in the blood is via hepatic metabolism. The half life determined for Norleual *in-vitro* (20.49 minutes) was relatively close to that determined *in-vivo* (28.0 minutes). The Cl_{int} value for Norleual obtained from the microsome study can be expressed per kilogram of body weight by adjusting for the protein content per gram of liver and the liver weight per kilogram of body weight in Sprague-Dawley rats (Naritomi, 2001). This extrapolation yields a Cl_{int} value of 0.121 L/min/kg. This value is higher than the CL value obtained *in-vivo* (0.057 L/min/kg). Such extrapolations more frequently underestimate actual (*in-vivo*) values, especially in high clearance drugs (Carlile, 1997).

3. 4. Discussion

This work is the first description of the physicochemical properties, metabolic stability and single-dose pharmacokinetics of Norleual, a putative c-Met receptor antagonist. Here we have described the basic metabolic and pharmacokinetic disposition of Norleual, including predicted physicochemical properties based on software simulation and plasma protein binding estimated by equilibrium dialysis. Experimental data showed a low level of plasma protein binding (albumin) for Norleual, which was opposite to the simulation results. Since our experiment was done using a solution of albumin only, this could mean that Norleual is highly bound to non-albumin plasma proteins.

Hepatic microsomal metabolism of Norleual was investigated using rat liver microsomes and indicated Norleual is metabolized by phase I enzymes. These data are in agreement with *in-vivo* pharmacokinetic data which indicated a relatively short half life. *In vitro-in vivo* correlation of data from the microsome and PK studies indicated that hepatic clearance is likely to be a major route of clearance of Norleual that is not degraded in the blood. However, since the half-life of Norleual in blood *in-vitro* is only 4.56 minutes, it is unlikely that a large fraction of the administered dose of Dihexa reaches the liver intact. Therefore, degradation of Norleual by blood enzymes is likely to be the primary mechanism of total body clearance.

The volume of distribution exhibited by Norleual was low, at 1.8 L/kg. A low volume of distribution indicates that Norleual resides primarily in the central blood compartment and is not well distributed into the tissues. Since Norleual is a potential anti-cancer therapeutic, this raises the concern that Norleual may not penetrate the interior of a well-established tumor at high

enough concentrations to impact its growth, particularly portions of the tumor that do not possess a strong blood supply. On the other hand, we have seen that Norleual induces strong physiological responses at very low concentrations, both *in-vitro* and *in-vivo* (Yamamoto 2010). Thus, a low penetrating fraction of Norleual may provide a suitable concentration for activity at the target site. Additionally, studies with murine cancer models indicate Norleual might be most effective as an anti-metastatic agent (Yamamoto 2010 and unpublished data). Therefore, penetration into deep layers of tumor tissue may not be necessary for Norleual efficacy. Alternatively, the low permeation of Norleual may also not be problematic in the treatment of tumors exhibiting the EPR (enhanced permeation and retention) effect. In fact, low permeation may prove to be beneficial in as much as the drug would not permeate deeply into healthy tissues and therefore toxic burdens within those tissues may be avoided. This would, however, mean that a large portion of the dose is more or less wasted. A chemical alteration that would increase in the lipophilicity of the molecule might result in a molecule more prone to penetrate membranous tissue barriers and consequently, a more efficient therapeutic that could be administered at lower doses.

These concerns are compounded by the short half life exhibited by Norleual. Because chemotherapy is typically chronic in nature, it could be highly impractical to administer doses of Norleual frequently enough to maintain relatively steady levels. Further, since Norleual does not appear to be a likely candidate for oral administration, it would likely be administered parenterally. This could result in the need for the patient to make frequent visits to or endure long stays at the hospital.

These concerns should be taken into consideration in determination of the potential of Norleual as a therapeutic agent. However, given the paucity of effective therapeutics available for many types of cancer, these concerns may be secondary in light of the efficacy of the agent.

CHAPTER FOUR

HIGH-PERFORMANCE LIQUID CHROMATOGRAPHIC ANALYSIS, PHARMACOKINETICS AND METABOLISM OF PNB-0405 IN RATS

4.1. Introduction

Recently published data from our laboratory indicate that angiotensin IV may exert its biological activity through the receptor tyrosine kinase, c-Met, which is known to play an important role in the development of a number of cancers. HGF is the only known ligand for c-Met and we have seen that our angiotensin IV analog AT_4 receptor antagonists are able to inhibit HGF-dependant cellular proliferation, invasion and scattering in several cell lines (Yamamoto 2010).

However, since these analogs are peptides, they inherently exhibit susceptibility to degradation by proteolytic enzymes and are therefore unstable in biological fluids. We have seen, with other angiotensin IV analogs such as Norleual, that this instability can be problematic, leading to short half-life in biological systems (McCoy unpublished). An extremely short half-life is impractical for potential drug candidates that will need to be administered chronically in order to treat long-term illnesses, such as cancer.

We have therefore developed angiotensin IV analogs with structural features that facilitate molecular stability and protect against proteolytic degradation. PNB-0405 is one such molecule with its c-terminal residues effectively protected by a 6-amino-hexamide moiety and

the use of the ‘d’ form of the n-terminal norleucine. These structural features endow the molecule with protection from amino- and carboxypeptidases and other enzymes.

Like Norleual, PNB-0405 has exhibited the ability to attenuate HGF-dependant cellular activities. PNB-0405 has been shown to inhibit HGF-dependant migration and scattering in MDCK cells (unpublished data). PNB-0405 also inhibits HGF-dependant association of Gab-1 (a scaffolding protein selective for c-Met) to the c-Met receptor (unpublished data).

Additionally, angiotensin IV/AT4 signaling is involved in vascular repair and remodeling, and inflammation, both processes that influence the growth and development of tumors. Recent research has also shown direct involvement of angiotensin IV in breast cancer (Pilar Carrera 2006) and pituitary tumors (Ochedalska 2002), and that AT4 is present in neuroblastoma cells (Mustafa 2001). In our laboratory, PNB-0405 inhibited tumor growth in a murine breast cancer model (unpublished data).

To confirm the increased stability of PNB-0405 compared to other angiotensin IV analogs and in order to develop optimal dosing strategies for further study of PNB-0405 anti-cancer activity, we wished to obtain basic knowledge of its metabolic and pharmacokinetic properties. An understanding of the basic pharmacokinetic parameters of PNB-0405 is also necessary for analysis of PNB-0405 as a therapeutic candidate and would be required for future implementation of phase I clinical trials. Therefore, we have investigated the physicochemical, metabolic and pharmacokinetic characteristics of PNB-0405 and present here a complete basic profile of PNB-0405 pharmacokinetic disposition.

In order to accurately analyze and quantify biological samples for *in-vivo* pharmacokinetic studies, it is necessary to develop and validate an assay that is accurate, precise

and reproducible. Here we also describe a method for extraction of PNB-0405 from serum and quantification of extracted PNB-0405 samples by tandem high-performance liquid chromatography – mass spectrometry.

4.2. Methods

4.2.1. Chemicals and Reagents

HPLC grade methanol, acetonitrile and water, and reagent grade trifluoroacetic acid were purchased from Sigma (St. Louis, MO, USA). PNB-0405 was synthesized in our lab.

4.2.2. Stock and Working Standard Solutions

PNB-0405 solutions were prepared in 30% ethanol at the concentrations specified. Stock PNB-0405 is kept in powder form and stored at -20ºC.

4.2.3. Microsomal Study

Male rat liver microsomes were obtained from Celsis (Baltimore, MD, USA). The protocol from Celsis for microsome-drug incubation was followed with minor adaptations. An NADPH regenerating system (NRS) was prepared as follows: 1.7 mg/mL NADP, 7.8 mg/mL glucose-6-phosphate and 6 units/mL glucose-6-phosphate dehydrogenase were added to 10 mL 2% sodium bicarbonate. The NRS was used immediately. 500 μM solutions of PNB-0405, piroxicam, (±)-verapamil and 7-ethoxycoumarin (low, moderate and highly metabolized controls, respectively) were prepared in acetonitrile. Microsomes were suspended in 0.1M Tris buffer (pH 7.38) at 0.5 mg/mL. 100 μL microsomes was added to pre-chilled microcentrifuge

tubes on ice. To each sample, 640 µL 0.1M Tris buffer and 10 µL 500 µM test compound were added. The samples and NRS were placed in a water bath at 37ºC for 5 minutes. The samples were removed from the water bath and 250 µL NRS was added to each. The samples were placed into a rotisserie hybridization oven at 37ºC with rotation at high speed for the appropriate incubation time (10, 20, 30 40 or 60 minutes). 500 µL from each sample was transferred to each of two tubes containing 500 µL ice-cold acetonitrile with internal standard per incubation sample. Standard curve samples were prepared in incubation buffer and 500 µL added to 500 µL ice-cold acetonitrile with internal standard. All samples were then analyzed by high performance liquid chromatography/mass spectrometry. Drug concentrations were determined and loss of parent relative to negative control samples containing no microsomes was calculated. Clearance was determined by nonlinear regression analysis for k_e and $t_{1/2}$ and the equation $Cl_{int} = k_e$ Vd.

4.2.4. Equilibrium Dialysis

The Rapid Equilibrium Dialysis (RED) kit was purchased from Thermo Scientific (Waltham, MA, USA). The kit protocol was followed. The base plate was rinsed in 20% ethanol for 10 minutes, then rinsed twice in distilled water and allowed to dry. RED inserts were placed in the base plate. 63µL of 1mg/mL PNB-0405 was added to an aliquot of 567 µL rat plasma. 200 µL from the plasma sample was transferred into each of three sample chambers, and 350 µL PBS was transferred into each of the corresponding buffer chambers. The plate was covered with sealing tape and incubated at room temperature on a shaker table over night. 50 µL from each chamber was transferred into clean microcentrifuge tubes. 50 µL PBS was added to the plasma

samples and 50 µL plasma was added to corresponding PBS samples. 300 µL ice-cold acetonitrile was added to each sample and the samples were held on ice for 30 minutes. The samples were centrifuged at 5000 RPM for 5 minutes and supernatants were transferred into clean tubes. The samples were then evaporated to dryness in a Savant SpeedVac® concentrator and reconstituted in 225 µL HPLC grade water and analyzed by high performance liquid chromatography according to the method described below.

4.2.5. Pharmacokinetic and Method Validation Sample Preparation

Fresh rat blood was obtained prior to each experiment via jugular vein catheters from adult male Sprague-Dawley rats. Quality control samples were prepared by spiking fresh rat blood on ice with an appropriate dilution of PNB-0405 in 30% ethanol for the final concentration of PNB-0405 specified, keeping a 10:1 ratio of blood to PNB-0405 solution.

The blood samples were immediately centrifuged at 5000 RPM for 5 minutes and a volume of serum equal to 0.4 times the sample blood volume is collected and transferred to new tubes. A $10^{-5.5}$ (w/v) dilution of PNB-0409, a molecule very similar in structure and properties to PNB-0405, was added to all serum samples at a volume equal to 0.1 times the volume of the serum sample as an internal standard. The proteins present in the serum samples were precipitated using 4 volumes of ice-cold acetonitrile, vortexed for approximately 10 seconds, and centrifuged at 5000 RPM for 5 minutes. The supernatants were transferred to new tubes and stored until use if necessary at 4ºC. The samples were then evaporated to dryness in a Savant

SpeedVac® concentrator. The residue was reconstituted in 225 µl 35% methanol and vortexed briefly, then transferred to autosampler vials.

4.2.6. Chromatographic System and Conditions

The HPLC/MS system used was from Shimadzu (Kyoto, Japan), consisting of a CBM-20A communications bus module, LC-20AD pumps, SIL-20AC auto sampler, SPD-M20A diode array detector and LCMS-2010EV mass spectrometer. Data collection and integration were achieved using Shimadzu LCMS solution software.

The analytical column used was an Econosphere C18 (100mm x 2.1mm) from Grace Davison Discovery Science (Deerfield, IL, USA). The mobile phase consisted of methanol and HPLC water with 0.1% trifluoroacetic acid. Separation was carried out using a non-isocratic method, starting at 40% methanol and climbing to 47% methanol over 3 minutes, and then to 49.73% at 7 minutes, at ambient temperature and a flow rate of 0.3 mL/min. For MS analysis, a positive ion mode (Scan) was used to monitor the m/z of PNB-0405 at 542 and the m/z of PNB-0409 (internal standard) at 436. Samples were introduced using the autosampler and the injection volume was 100ul. For the microsomal study, the m/z of (±)-verapamil was 455, the m/z of piroxicam was 332, and the m/z of 7-ethoxycoumarin was 191.

4.2.7. Method Validation

4.2.7.1. Recovery

Recovery of PNB-0405 from biological fluids was assessed (n = 3) at 100ug/mL by spiking blood samples with PNB-0405. Samples were then prepared as described above (Sample Preparation). The LCMS response for these samples was compared to that of freshly prepared samples of PNB-0405 in 35% methanol.

4.2.7.2. Selectivity

Selectivity was assessed using chromatograms from samples used for the precision and accuracy experiment. Selectivity was evaluated by peak purity analysis.

4.2.7.3. Precision and Accuracy

PNB-0405 precision and accuracy was determined by preparation of four sets of four concentrations of PNB-0405 in blood (0.01, 0.1, 1 and 10 ug/mL). Each of the four sets of QC samples was prepared separately from scratch. Samples were prepared by spiking blood aliquots with PNB-0405 and processing as described above (Section 4.2.5). The between-run precision and accuracy of the assays were estimated using the results from each set of samples to quantify another set.

4.2.7.4. Lower Limit of Quantification

The lower limit of quantification (LLOQ) was determined as the lowest concentration of PNB-0405 that could be quantified with an average bias of less than 25%.

4.2.7.5. Stability Studies

To determine the stability of PNB-0405 in blood, PNB-0405 was spiked into blood (n=3 per time point, except at 5 hours, n=2) and the samples placed in an incubator at 37ºC. At zero, 1, 3, and 5 hours, a set of samples was removed from the incubator and prepared for high-performance liquid chromatography as described above.

4.2.8. Pharmacokinetic Studies

4.2.8.1. Animals and Surgical Procedures

Male Sprague-Dawley rats (250+ g) were obtained from Harlan Laboratories (CA, USA) and allowed food (Harlan Teklad rodent diet) and water *ad libitum* in our animal facility. Ethics approval for animal experimentation was obtained from Washington State University. Rats were housed in temperature-controlled rooms with a 12 hour light/dark cycle. The right jugular veins of the rats were catheterized with sterile polyurethane Hydrocoat™ catheters (Access Technologies, Skokie, IL, USA) under ketamine (Fort Dodge Animal Health, Fort Dodge, IA, USA) and isoflurane (Vet One™, MWI, Meridian, ID, USA) anesthesia. The catheters were exteriorized through the dorsal skin. The catheters were flushed with heparinized saline before

and after blood sample collection and filled with heparin-glycerol locking solution (6 mL glycerol, 3 mL saline, 0.5 mL gentamycin (100mg/mL), 0.5 mL heparin (10,000 u/mL)) when not sampled for more than 8 hours.

4.2.8.2. Pharmacokinetic Study

Male Sprague Dawley rats were catheterized as described in the Animals and Surgical Procedures section. The animals were placed in metabolic cages prior to the start of the study and time zero blood samples were collected. The animals were then dosed intravenously via the jugular vein catheters or subcutaneously with PNB-0405 (24 mg/kg) suspended in 30% ethanol. After dosing, blood samples were collected as follows (times and blood volumes collected are listed in chronological order):

Compound	**Dosage Route**	**Time (minutes)**	**Blood Volume Collected (µl)**
PNB-0405	Intravenous	0, 12, 30, 60, 90, 120, 180, 240, 300	200, 200, 200, 200, 200, 300, 400, 500, 500
	Subcutaneous	0, 15, 30, 60, 120, 180, 240, 360, 420, 540	200, 200, 200, 200, 200, 200, 300, 400, 500, 500

After each blood sample was taken, the catheter was flushed with heparinized saline or heparinized Ringer's solution and a volume of heparinized saline or Ringer's equal to the volume of blood taken was injected (to maintain total blood volume).

4.3. Results and Interpretation

4.3.1. Method Validation

4.3.1.1. Selectivity and Chromatography

Good separation of PNB-0405 and the internal standard in serum was successfully achieved. No interfering peaks co-eluted with the analyte or internal standard (Figure 4.1). Peak purity analysis revealed a peak purity index for PNB-0405 of 0.95 and the internal standard of 0.94. PNB-0405 eluted at 5.06 minutes and the internal standard at 4.31 minutes.

In order to determine the best chromatographic method for separation and resolution of PNB-0405 and the internal standard, optimization of the mobile phase gradient was performed. The addition of 0.1% (v/v) trifluoroacetic acid (TFA) was used as an ion-pairing agent. The organic phase (methanol 0.1% TFA) gradient was tested revealing an optimal organic gradient of 40 to 47 percent over 3 minutes and 47 to 49.73 percent from 3 to 7 minutes. Additionally, the flow rate was optimized to an optimum flow rate of 0.3mL/min. These settings provided optimal separation and peak shape with minimal run time.

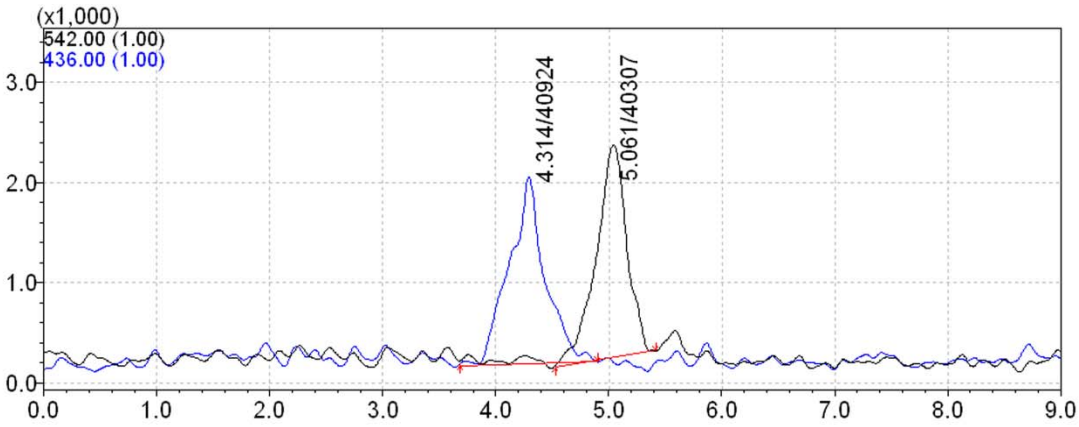

Figure 4.1. Representative chromatogram of PNB-0405 (m/z 542) and the internal standard (m/z 436) recovered from rat serum. The chromatographic conditions consisted of an Econosphere C18 (100mm x 2.1mm) column and mobile phase consisting of methanol and water with 0.1% trifluoroacetic acid. Separation was carried out using a gradient starting at 40% methanol and increasing to 49.73% methanol over 7 minutes at ambient temperature and flow rate of 0.3 mL/min.

4.3.1.2. Recovery

The recovery of PNB-0405 from blood by acetonitrile protein precipitation was evaluated using three replicate samples, each, PNB-0405 spiked in blood (n = 3) or 35% methanol (n = 3) (100ug/mL). The mean extraction efficiency of this method for PNB-0405 was 35.77% ± 8.23% (standard deviation).

4.3.1.3. Precision and Accuracy

Table 4.1 shows within- and between-run precision and accuracy for the determination of PNB-0405 concentrations in serum. The method demonstrated fair accuracy. The within- and between-run bias for the determination of PNB-0405 concentrations in serum was less than 20%, except below the LLOQ (0.1 ug/mL). The maximum deviation of estimated values from actual values within the LLOQ was 7.92% within-run, and 19.08% between-runs. Precision (R.S.D.) values were below 20% for within-run calculations. R.S.D. values for between-run calculations were higher but below 45%. These data indicate that the method is adequately accurate and reproducible for preliminary studies providing basic pharmacokinetic parameters for PNB-0405.

Table 4.1 Within- and between-run precision and accuracy of the assay for PNB-0405 in serum (n = 4, mean ± SD)

Concentration (µg/mL)	**Precision (average ± SD)**		**Accuracy**			
	Within-run	**Between-run**	**Within-run**		**Between-run**	
	(µg/mL)	**(µg/mL)**	**%**	**Bias (%)**	**%**	**Bias (%)**
10	9.83 ± 0.34	8.09 ± 2.68	98.28	-1.72	80.92	-19.08
1	1.02 ± 0.03	1.10 ± 0.49	101.50	1.50	109.93	9.93
0.1	0.09 ± 0.02	0.10 ± 0.02	92.08	-7.92	97.16	-2.84

4.3.1.4. Curve-Fit and LLOQ

The relationship between concentration and response was fit to a sigmoidal equation with an r^2 value of ≥ 0.99. The lower limit of quantification (LLOQ) for the determination of PNB-0405 concentrations in serum was 0.1 μg/mL. This is the lowest concentration that could be quantified with an average bias of less than 20%.

4.3.1.5. Stability

The stability of PNB-0405 in blood was assessed (n = 3) by comparing samples of PNB-0405 spiked in blood and incubated at 37º C for 0, 1, 3 and 5 hours (Figure 4.2). There was a 19.88% reduction in response between zero hour and one hour blood samples; another 14.74% reduction in response between one hour and three hour blood samples; and a 7.82% reduction in response between three hour and five hour samples. These data indicate that PNB-0405 is unstable in the blood at 37ºC, likely owing to metabolism by plasma enzymes. However, as expected, PNB-0405 appears to be significantly more stable in blood than other angiotensin-IV analogs with anti-cancer activity that we have investigated in our lab (McCoy unpublished). The calculated stability $t_{1/2}$ based on a single phase exponential decay was 1.24 hours ($r^2 = 0.95$) however this value does not represent the real biological half life of PNB-0405 in blood due to the fact that the curve does not extend to the point at which the blood level of PNB-0405 was at or near zero.

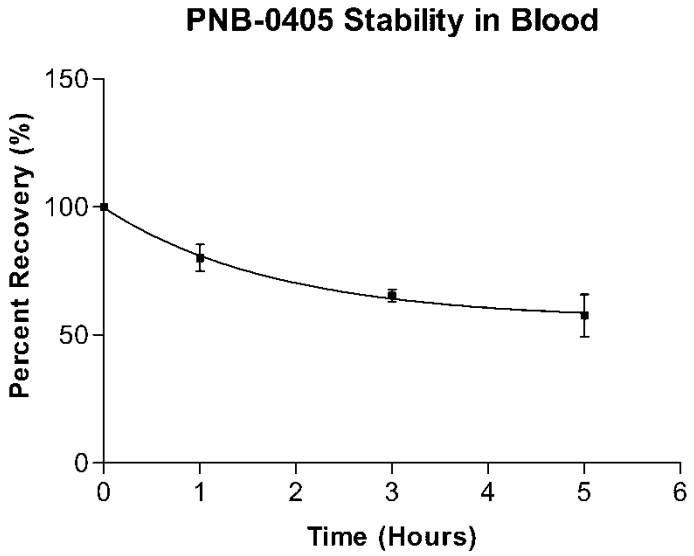

Figure 4.2 Stability of PNB-0405 in rat blood stored at 37º C (n = 3). Percent recovery over time (mean ± SD).

4.3.2. Pharmacokinetics and Metabolism

4.3.2.1. Modeling of Physicochemical Properties and Plasma Protein Binding

In order to determine basic physicochemical properties of PNB-0405, the molecule was modeled using ADMET Predictor® software (Simulations Plus Inc., Lancaster, CA, USA). Table 4.2 shows the resulting values for parameters of interest.

Table 4.2. Predicted Physicochemical Properties of PNB-0405

Physicochemical Property	**Predicted Value**
logP	1.45
P_{eff}	1.53
P_{avg}	0.39
Pr_{Unbnd}	42.68

It is important to note that software modeling of molecules is a useful tool that can provide an estimation of actual values but should not be considered as an equivalent substitute for experimental determination of these properties. Information on the accuracy of ADMET Predictor® modeling algorithms can be found at the company website.

The logP value represents the log transformation of the octanol-water partition coefficient and is a measure of hydrophilicity. The predicted logP value of 1.45 indicates that PNB-0405 partitions into octanol at a rate of 28.18 mol for every 1 mol that partitions into water. This indicates that PNB-0405 is relatively hydrophobic. Hydrophobicity is an important parameter for permeation of compounds across membranes and can, in part, determine the ability of a molecule to permeate the walls of the gastro-intestinal tract. The P_{eff} value represents the predicted effective human jejunal permeability of the molecule. The predicted P_{eff} value for PNB-0405 (1.53) is intermediate between the predicted P_{eff} values for enalapril (1.25) and piroxicam (2.14), two orally bioavailable drugs in use in the clinic. The P_{avg} value represents the approximate average intestinal permeability along the entire human intestinal tract. The predicted P_{avg} value for PNB-0405 is 0.39. This value is lower than the predicted values for other orally available drugs used for comparison.

Pr_{Unbnd} stands for percent unbound and indicates the percent of PNB-0405 not bound to plasma proteins in circulation. PNB-0405 was predicted to be 42.68% unbound to plasma proteins. The percent PNB-0405 unbound to plasma proteins as determined by equilibrium dialysis was 68.49 ± 9.49 %.

4.3.2.2. *In-vivo* Pharmacokinetics Studies

Relevant pharmacokinetic parameters of PNB-0405 after single intravenous (IV) and subcutaneous (SC) bolus dosing (24 mg/kg) in rats are summarized in Tables 4.3 and 4.4, respectively. Serum data were modeled using WinNonlin® software to perform non-compartmental analysis. The half life ($t_{1/2}$) of PNB-0405 after IV dosing was determined to be 1012 ± 391.4 minutes. PNB-0405 was extensively distributed outside the central blood compartment after IV dosing as evidenced by its large volume of distribution (Vd) of 104,186.8 ± 65,034.3 L/kg. Total body clearance of PNB-0405 from serum as determined after IV dosing was 58.3 ± 15.6 L/min/kg. Area under the curve (AUC), a measure of total drug exposure, was determined to be 692.5 ± 293.2 min.ng/mL after IV dosing, and 178.0 ± 41.7 min.ng/mL after SC dosing. Both of these AUC values are assumed to be underestimated due to limited assay sensitivity.

Table 4.3. PK parameters of PNB-0405 following single-dose IV administration in rats (n = 5).

Pharmacokinetic Parameter	**Mean**	**±**	**SEM**
$AUC_{0-\infty}$ (min.ng/mL)	692.5	±	293.2
Vd (L/kg)	104186.8	±	65034.3
C_p^0 (ng/mL)	68.2	±	32.2
$t_{1/2}$ (min)	1012.0	±	391.4
KE (min^{-1})	0.001	±	0.0002
CL (L/min/kg)	58.3	±	15.6

Table 4.4. PK parameters of PNB-0405 following single-dose SC administration in rats (n = 5).

Pharmacokinetic Parameter	**Mean**	**±**	**SEM**
$AUC_{0-\infty}$ (min.ng/mL)	178.0	±	41.7
C_{max} (ng/mL)	0.83	±	0.24
F (% Bioavailability)	25.7		

The serum concentration-time profile for PNB-0405 after a single IV bolus dose was biphasic (Figure 4.3). Serum concentrations declined rapidly from 12 to 90 minutes during an apparent distribution phase, followed by a pure elimination phase in which serum concentrations declined more slowly. Serum concentrations were below the limit of detection after 240 minutes.

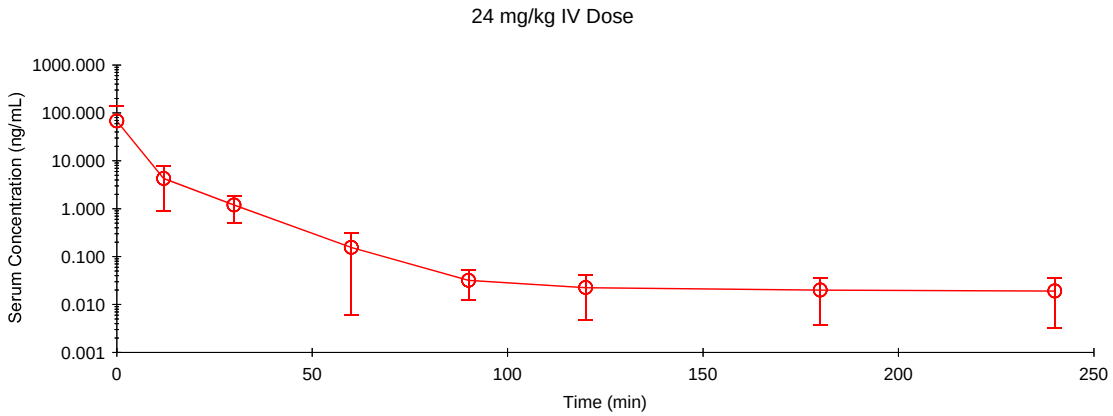

Figure 4.3 Serum concentration-time profile following a single 24 mg/kg IV dose of PNB-0405. Mean ± SD, n = 5.

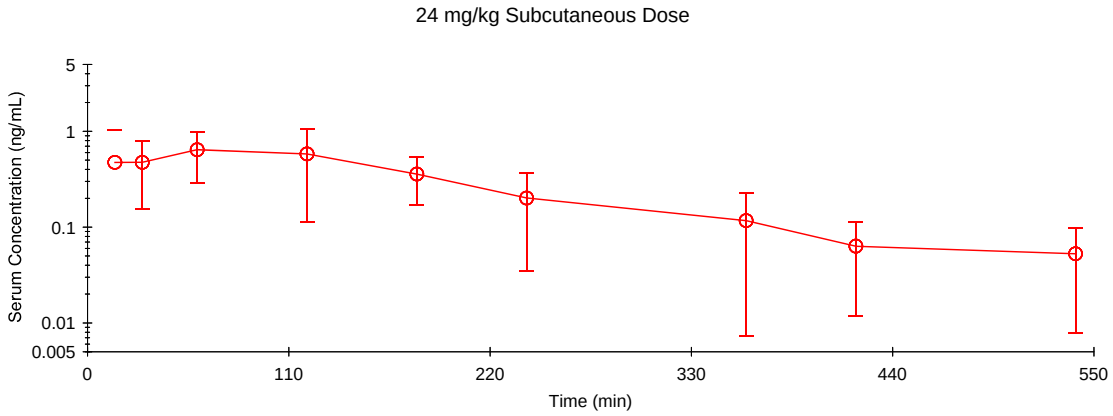

Figure 4.4 Mean serum drug concentration-time profile following a single 24 mg/kg SC dose of PNB-0405. Mean ± SD, n = 5.

After SC dosing, the serum concentration-time profile of PNB-0405 exhibited a short absorption phase with serum concentrations increasing from 0 to 60 minutes. Serum levels plateaued from 60 to 120 minutes as absorption occurred at approximately the same rate as distribution and elimination, combined. Serum concentrations of PNB-0405 after SC dosing were below the limit of quantification after 540 minutes but the pure elimination phase of the serum concentration/time curve had not yet been reached (Figure 4.4). It appears that absorption is the rate-limiting factor of total body clearance of PNB-0405 up to 420 minutes after SC dosing (i.e. "flip-flop" kinetics). Thus, the slope of the concentration/time curve represents, both, the absorption rate constant (k_a) and the elimination rate constant (k_e). The rate of absorption of PNB-0405 after SC dosing is slow, probably owing to travel through the lymphatics in addition to direct absorption into capillaries. Another possibility is that PNB-0405 came out of solution in the aqueous environment upon subcutaneous injection, which would also slow absorption. From 420 to 540 minutes, it appears that the rate of clearance from the serum may have begun to slow in what may have been the beginning of the pure elimination phase. Bioavailability of PNB-0405 after SC dosing was determined to be 25.7% ($AUC_{SC}/AUC_{IV}*100$).

4.3.2.3. Intrinsic Clearance of PNB-0405 in Rat Liver Microsomes

The phase I metabolism of PNB-0405 was tested in male rat liver microsomes with no apparent loss of parent molecule. Piroxicam, (±)-verapamil and 7-ethoxycoumarin were also tested as low, moderate and highly metabolized (respectively) reference compounds. The reference compounds exhibited intrinsic clearance values that were within the range of values

found in the literature. This result suggests that PNB-0405 does not undergo phase I metabolism. However, the maximum time for incubation of microsome samples is 90 minutes. Therefore, it is possible that PNB-0405 undergoes phase I metabolism but at very slow rate not detectable with the assay.

4.4. Discussion

We have described here the validation of an assay for the extraction and quantification of PNB-0405 in serum. There is currently no other assay for detection of PNB-0405 in serum published in the literature. The method presented here is practical and efficient and provides a validated means of determining PNB-0405 concentrations in the serum for use in pre-clinical studies. It would, however, be desirable to develop an assay that exhibits greater accuracy and precision at lower concentrations of PNB-0405. Such an assay would allow for more accurate determination of PNB-0405 pharmacokinetic parameters since it would allow for detection of PNB-0405 at later post-dose time points.

This work is also the first description of single-dose pharmacokinetics of angiotensin IV analog, PNB-0405, a putative antagonist of c-Met receptor signaling. We have presented the physicochemical properties of PNB-0405 based on software modeling, which describe PNB-0405 as a hydrophobic molecule predicted to have moderate oral bioavailability and to exhibit moderate plasma protein binding. Equilibrium dialysis studies also indicate that PNB-0405 binds to plasma proteins. Experimentally, the ratio of plasma protein binding for PNB-0405 is 68.49% bound. These results are expected to be more accurate than the modeling estimation.

Studies using rat liver microsomes were unable to show any phase I metabolism of PNB-0405 even though the intrinsic clearance values of reference compounds were determined with good results. We have also shown the *in-vivo* pharmacokinetics of PNB-0405 after intravenous and subcutaneous dosing. These studies estimate the in-vivo half life of PNB-0405 at 1012 min (16.87 hours, based on IV dosing data). The volume of distribution was 104,186.8 L/kg (based

on IV dosing data), indicating extensive distribution of PNB-0405 out of the central blood compartment and into the tissues (given that the estimated total blood volume of a rat is 0.062 L/kg, Lee 1985).

Thus, we have shown that the exchange of the three c-terminal amino acids of angiotensin IV for the non-amino-acid moiety, 6-aminohexamide, and the use of the 'd' form of the norleucine in the first position, provide protection from enzymatic degradation and increases the *in-vitro* and *in-vivo* half life. The increase in half life *in-vivo* is roughly 36-fold compared to Norleual, our other angiotensin IV analog with therapeutic potential as an anti-cancer agent, which does not have either of these modifications. The 6-aminohexamide moiety also endows the molecule with increased lipophilicity while retaining the small size of the molecule. These characteristics endow the molecule with increased ability to penetrate into the tissues, increasing the likelihood that a substantial fraction of the administered dose will reach the target site. The increased permeability of the molecule is also evidenced by the modeling prediction of possible oral bioavailability.

These data support the conclusion that PNB-0405 exhibits pharmacokinetic properties that make it practical for use in the clinic and a good candidate for further investigation as a potential therapeutic agent.

CHAPTER FIVE

HIGH-PERFORMANCE LIQUID CHROMATOGRAPHIC ANALYSIS, PHARMACOKINETICS AND METABOLISM OF DIHEXA IN RATS

5.1. Introduction

In 2005, a Delphi consensus study estimated the prevalence of dementia at 3 percent of the North American population between the ages of 70 and 74, increasing to 30 percent over the age of 85. This equates to 53.1 million people living with dementia in North America, alone (Ferri 2005). Yet there remains no effective therapy for loss of memory or other cognitive functions.

Angiotensin IV-AT_4 receptor signaling is well known to improve cognitive function in cognitive deficit animal models (Braszko 2006, Albiston 2004, Lee 2004, Wright 2004 review) and in long-term potentiation studies, a putative measure of learning activity in the brain (Davis 2006, Wayner 2001, Kramar 2001). Therefore, it is reasonable to investigate the angiotensin IV-AT_4 system as a potential target for development of new therapies for Alzheimer's and other neurodegenerative disorders. However angiotensin IV is a peptide hormone and is therefore highly susceptible to degradation by proteolytic enzymes to products unlikely to have specific physiological activity. Consequently, its usefulness as an exogenous pharmaceutical agent is limited.

Our laboratory has developed a number of angiotensin IV analogs with good affinity and potent activity at the AT_4 receptor (Krebs 1996, Wright 1999, Kramar 2001). We have recently synthesized a new angiotensin IV analog, "Dihexa" (a.k.a. PNB-0408). Dihexa has been shown

to increase long-term potentiation in hippocampal neurons and to improve cognitive function in the scopolamine model of cognitive deficit and in aged animals as tested in the Morris water maze task of spatial learning (unpublished data). Dihexa is effectively protected at both the n- and c- terminus by synthetic moieties, making it much less susceptible to enzymatic degradation and therefore suitable for exogenous administration. Angiotensin IV contains a valine in the first position, which has been replaced with a hexanoic-acid moiety for Dihexa. Additionally, the three c-terminal residues of angiotensin IV have been replaced with a 6-aminohexamide moiety (Table 5.1). These two non-amino acid moieties retain the basic structural and physicochemical features of the replaced residues necessary for binding to the AT_4 receptor, yet limit the ability of amino- and carboxypeptidases to cleave n- or c-terminal residues (respectively).

Table 5.1 Structural modifications of angiotensin IV to produce Dihexa and the internal standards.

Name	**Structure**
Angiotensin IV	Val-Tyr-Ile-His-Pro-Phe
Dihexa	Hexanoic-Tyr-Ile-(6)aminohexamide
PNB-0407 (Internal Standard)	Valeric-Tyr-Ile-(6)aminohexamide
PNB-0412 (Internal Standard)	Heptanoic-Tyr-Ile-(6)aminohexamide

Activation of the c-Met receptor by its ligand hepatocyte growth factor (HGF) has also been shown to improve cognitive function in certain paradigms, including a murine model of Alzheimer's disease (Takeo 2007, Takeuchi 2008). Further, c-Met activation has been shown to

be neurotrophic (Honda 1995, Ebens 1996, Kadoyama 2007). In addition to being a stable angiotensin IV analog, Dihexa has also exhibited c-Met agonist activity in Western blots of c-Met associated Gab-1 (a c-Met specific scaffolding protein) after immunoprecipitation (unpublished data).

In order to determine whether Dihexa exhibits a pharmacokinetic disposition that will be practical for use as a therapeutic agent, we wished to conduct studies to establish its basic pharmacokinetic parameters. To this end, we have developed and validated an analytical method by which Dihexa concentrations in plasma can be determined consistently and accurately. This method was used to investigate the pharmacokinetics of Dihexa after intravenous, intraperitoneal and oral dosing. We have also investigated the phase I metabolism of Dihexa using rat liver microsomes.

Here we report the validation of a simple, selective, reversed-phase HPLC/mass spectrometry assay for the detection of Dihexa in plasma and urine. Further, we describe the basic pharmacokinetic disposition of Dihexa, including physicochemical properties, metabolism and intraperitoneal bioavailability.

5.2. Methods

5.2.1. Chemicals and Reagents

Heparin sodium salt, sodium bicarbonate, dimethyl sulfoxide (DMSO), dimethyl formamide, glycerol, propylene glycol, polyethylene glycol, glycine, sodium citrate, HPLC grade ethanol, acetonitrile and water, and reagent grade formic and acetic acid were purchased from Sigma (St. Louis, MO, USA). β-Cyclodextrin was purchased from TCI America (Portland, OR, USA). Phosphate buffered saline (PBS) was purchased from BioRad (Hercules, CA, USA). Tris base was purchased from Fisher (Fair Lawn, NJ, USA). Dihexa was synthesized in our laboratory.

5.2.2 Microsomal Study

Male rat liver microsomes were obtained from Celsis (Baltimore, MD, USA). The protocol from Celsis for microsome-drug incubation was followed with minor adaptations. An NADPH regenerating system (NRS) was prepared as follows: 1.7 mg/mL NADP, 7.8 mg/mL glucose-6-phosphate and 6 units/mL glucose-6-phosphate dehydrogenase were added to 10 mL 2% sodium bicarbonate. The NRS was used immediately. 500 μM solutions of Dihexa, piroxicam, (±)-verapamil and 7-ethoxycoumarin (low, moderate and highly metabolized controls, respectively) were prepared in acetonitrile. Microsomes were suspended in 0.1M Tris buffer (pH 7.38) at 0.5 mg/mL. 100 μL microsomes was added to pre-chilled microcentrifuge

tubes on ice. To each sample, 640 µL 0.1M Tris buffer and 10 µL 500 µM test compound were added. The samples and NRS were placed in a water bath at 37ºC for 5 minutes. The samples were removed from the water bath and 250 µL NRS was added to each. The samples were placed into a rotisserie hybridization oven at 37ºC with rotation at high speed for the appropriate incubation time (20, 30 40, 60 or 90 minutes). 500 µL from each sample was transferred to each of two tubes containing 500 µL ice-cold acetonitrile with internal standard per incubation sample. Standard curve samples were prepared in incubation buffer and 500 µL added to 500 µL ice-cold acetonitrile with internal standard. All samples were then analyzed by high performance liquid chromatography/mass spectrometry. Drug concentrations were determined and loss of parent relative to negative control samples containing no microsomes was calculated. Clearance was determined by nonlinear regression analysis for k_e and $t_{1/2}$ and the equation $Cl_{int} = k_e$ Vd.

5.2.3. Pharmacokinetic and Method Validation Sample Preparation

Fresh rat blood was obtained prior to each experiment via jugular vein catheters from adult male Sprague-Dawley rats.

Dihexa solutions were prepared by suspending dry stock Dihexa in DMSO at 1mg/mL and subsequent serial dilutions in 50% DMSO or HPLC grade water for the final concentrations specified. Stock Dihexa is kept in powder form and stored at -20ºC. Quality control (QC) samples were prepared by spiking fresh rat plasma or urine with an appropriate dilution of Dihexa for the final concentration of Dihexa specified, keeping a 10:1 ratio of plasma or urine to Dihexa solution. The compounds, PNB-0407 and PNB-0412, both molecules very similar in

structure (Table 5.1 shows structure) and properties to Dihexa, were used as internal standards and were prepared the same way.

The proteins present in the plasma samples were precipitated using 3 volumes of ice-cold acetonitrile. Internal standard PNB-0407 was then added and the samples vortexed for approximately 10 seconds. The samples were then centrifuged at 5000 RPM for 5 minutes. The supernatants were transferred to new tubes and stored until use if necessary at -20ºC. The samples were then concentrated in a Savant SpeedVac® concentrator to a volume of approximately 100ul. 200ul HPLC grade water was added to each sample and the samples were transferred to autosampler vials.

Urine samples were processed as follows. Internal standard PNB-0412 was added to urine samples, which were then concentrated in a Savant SpeedVac® concentrator to a volume of approximately 10-25ul. 50ul ice-cold acetonitrile was then added, the samples were vortexed for approximately 10 seconds and centrifuged at 5000 RPM for 5 minutes. Supernatants were transferred to autosampler vials containing 100ul HPLC grade water.

5.2.4 Pharmacokinetic Study

Male Sprague Dawley rats were catheterized as described in the Animals and Surgical Procedures section. The animals were placed in metabolic cages prior to the start of the study and time zero blood and urine samples were collected. The animals were then dosed intravenously via the jugular vein catheters, intraperitoneally, or orally with Dihexa dissolved in

75% DMSO (except for the 45 mg/kg oral dose study for which Dihexa was suspended in distilled water) at the dose specified. After dosing, blood samples were collected as follows:

Dosage Route	**Dose**	**Blood Sample Volume**	**Sample Collection Times (minutes unless otherwise noted)**
Intravenous	10 mg/kg	200 μL	0, 10, 30, 90, 150, 240, 330, 420, 510, 600, 690, 780, 24 hours, 48 hours, 5 days
Intraperitoneal	20 mg/kg	200 μL	0, 10, 30, 60, 90, 120, 150, 180, 240, 300, 360, 420, 480, 600, 720, 24 hours, 48 hours, 5 days
Oral	10 mg/kg	200 μL	0, 10, 20, 30, 60, 90, 120, 150, 180, 240, 300, 360, 420, 480, 600, 720, 24 hours, 48 hours, 5 days
Oral	45 mg/kg	3 mL	1 hour, 3 hours, 5 hours

After each blood sample was taken, the catheter was flushed with heparinized lactated Ringer's solution and a volume of heparinized lactated Ringer's equal to the volume of blood taken was injected (to maintain total blood volume). Urine samples were collected depending on when the animals urinated and ensuring that there was a blood sample collected at the midpoint between urine collections. Coolers for the urine collection tubes were utilized so that urine remained ice-cold until collected. Urine samples were stored at -20ºC until further processing.

The blood samples (except for the 45 mg/kg oral dose study samples) were collected into polypropylene microcentrifuge tubes and cooled on ice for not more than 1 hour. The samples were centrifuged at 5000 RPM for 7 minutes and 80 µL plasma were transferred into previously prepared tubes containing 240 µL ice-cold acetonitrile. The samples were vortexed vigorously for 30 seconds and held on ice. 10 µL 100 µg/mL PNB-0407, another compound from our library used as an internal standard, was added to each sample on ice. Samples were held on ice until the end of the experiment and stored at -20ºC afterward until further processing.

Serial dilutions of Dihexa in 50% DMSO or water (for dilutions of 50 µg/mL or less) were prepared from the stock used to dose the animals to be used for preparation of a standard curve. 10 µL of each serial dilution was then added to 90 µL of blank plasma for final concentrations of 0.01, 0.02, 0.05, 0.1, 0.2, 1, 10, 20 and 100 µg/mL. 80 µL of each plasma sample was transferred to previously prepared tubes containing 240 µL ice-cold acetonitrile and vortexed vigorously. 10 µL 100 µg/mL PNB-0407, as an internal standard, was added to each sample on ice. The standard curve plasma samples were then stored at -20ºC and further processed alongside the pharmacokinetic study samples according to the method described in section 2.3.

For the 45 mg/kg oral dose study, an animal was anesthetized at each time point and 3 mL blood were taken by cardiac puncture. The animals were subsequently sacrificed. The blood was collected into heparinized vacutainer tubes and centrifuged at 2600g for 5 minutes. 1.2 mL plasma was transferred to new vials and 3 volumes ice-cold acetonitrile were added along with internal standard. The samples were transferred to microcentrifuge tubes 1 mL at a time and concentrated in a Savant SpeedVac® concentrator to a volume of approximately 100µL. 200ul

HPLC grade water was added to each sample and the samples were transferred to autosampler vials and analyzed by LC/MS.

The previously prepared stock dilutions of Dihexa prepared from the solution used to dose the animals (above) were used to prepare urine standard curves. 10 µL of each serial dilution was added to 90 µL of blank urine for final concentrations of 0.02, 0.1, 1, 10 and 100 µg/mL. 10 µL 100 µg/mL internal standard, PNB-0412, was added to each. The standard curve samples were then stored at -20ºC and further processed alongside the pharmacokinetic study urine samples.

Total urine volumes collected for each time point were measured and recorded and 100 µL from each sample was transferred to a clean microcentrifuge tube. 10 µL 100 µg/mL internal standard, PNB-0412, was added to each. Samples were further processed according to the method described in section 2.3.

5.2.5. Chromatographic System and Conditions

The HPLC/MS system used was from Shimadzu (Kyoto, Japan), consisting of a CBM-20A communications bus module, LC-20AD pumps, SIL-20AC auto sampler, SPD-M20A diode array detector and LCMS-2010EV mass spectrometer. Data collection and integration were achieved using Shimadzu LCMS solution software.

The analytical column used was an Econosphere C18 (100mm x 2.1mm) from Grace Davison Discovery Science (Deerfield, IL, USA). The mobile phase consisted of HPLC grade acetonitrile (ACN) and water with 0.1% acetic acid. For plasma samples, separation was carried

out using a non-isocratic method, starting at 23% ACN and climbing to 31% ACN over 9 minutes, at ambient temperature and a flow rate of 0.3 mL/min. For urine samples, separation was carried out using a non-isocratic method, starting at 23% ACN and climbing to 35% ACN over 9 minutes. For MS analysis, a positive ion mode (SIM) was used to monitor the m/z of Dihexa at 527 (Dihexa with the addition of a sodium adduct) and the m/z of PNB-0407 and PNB-0412 (internal standards) at 513 and 541, respectively (both with sodium adducts). Samples were introduced using the autosampler and the injection volume was 50ul. For the microsomal study, the m/z of (±)-verapamil was 455, the m/z of piroxicam was 332, and the m/z of 7-ethoxycoumarin was 191.

5.2.6. Animals and Surgical Procedures

Male Sprague-Dawley rats (250+ g) were obtained from Harlan Laboratories (CA, USA) and allowed food (Harlan Teklad rodent diet) and water *ad libitum* in our animal facility. Ethics approval for animal experimentation was obtained from Washington State University. Rats were housed in temperature-controlled rooms with a 12 hour light/dark cycle. The right jugular veins of the rats were catheterized with sterile polyurethane Hydrocoat™ catheters (Access Technologies, Skokie, IL, USA) under ketamine (Fort Dodge Animal Health, Fort Dodge, IA, USA) and isoflurane (Vet One™, MWI, Meridian, ID, USA) anesthesia. The catheters were exteriorized through the dorsal skin. The catheters were flushed with heparinized saline before and after blood sample collection and filled with heparin-glycerol locking solution (6 mL

glycerol, 3 mL saline, O.5 mL gentamycin (100mg/mL), 0.5 mL heparin (10,000 u/mL)) when not sampled for more than 8 hours.

5.2.7. Pharmacokinetic Analysis

Pharmacokinetic analysis was performed using data from individual rats from which the mean and standard deviation were calculated for each group. Noncompartmental pharmacokinetic parameters were calculated from plasma drug concentration-time profiles by use of WinNonlin® software (Pharsight, Mountain View, CA, USA). The following relevant parameters were determined where possible: area under the concentration-time curve from time zero to the last time point ($AUC_{0\text{-}last}$) or extrapolated to infinity ($AUC_{0\text{-}\infty}$), C_{max} concentration in plasma extrapolated to time zero (C_0), terminal elimination half-life ($t_{1/2}$), volume of distribution (Vd), and clearance (CL). Urine concentrations were determined and relevant parameters were calculated, including total amount excreted, excretion rate, amount remaining to be excreted and renal clearance.

5.2.8. Method Validation

5.2.8.1. Recovery

Recovery of Dihexa from blood and plasma was assessed (n = 3) at 5 concentrations (0.01, 0.1, 1, 10 and 100 ng/mL) by spiking blood, plasma and water samples with Dihexa

suspended in DMSO and acetonitrile. Samples were then prepared as described above (section 5.2.3). The LCMS response for the blood and plasma samples was compared to that of the water samples.

Recovery of Dihexa from urine was assessed (n = 3) at seven concentrations (0.1, 0.2, 1, 10, 20, 50 and 100 ug/mL) by spiking urine samples with Dihexa stock solutions prepared as described above. Urine samples were then prepared for chromatography as described above (section 5.2.3). The LCMS response for these samples was compared to that of a freshly prepared sample Dihexa in water at the same concentrations.

5.2.8.2. Selectivity

Selectivity was assessed using chromatograms from samples used for the precision and accuracy experiment. Selectivity was evaluated by peak purity analysis at 280nm.

5.2.8.3. Precision and Accuracy

Dihexa precision and accuracy was determined by preparation of three sets of six concentrations of Dihexa in plasma (0.05, 0.1, 1, 10 and 100 ug/mL) and urine (0.02, 0.1, 1, 10 and 100 ug/mL). Each of the three sets of QC samples was prepared separately. Samples were prepared by spiking plasma or urine aliquots with Dihexa and processing as described above (section 2.2). The between-run precision and accuracy of the assays were estimated using the results from each set of samples to quantify the other two sets.

5.2.8.4. Lower Limit of Quantification

The lower limit of quantification (LLOQ) was determined as the lowest concentration of Dihexa that could be quantified with an average bias of less than 20%.

5.2.8.5. Stability Studies

The stability of Dihexa stock solutions stored in the autosampler rack (15ºC) was evaluated over 9 days. For these studies, the stability was evaluated by comparing the peak area ratio of Dihexa to PNB-0407 in stored samples at 1, 3 and 9 days.

To determine the stability of Dihexa in acetonitrile at -20ºC, Dihexa and was spiked into HPLC grade acetonitrile (n = 3) and the samples stored at -20ºC for zero, 16, and 64 hours. At each time point, an aliquot was taken from the samples for analysis by high performance liquid chromatography. For this study, the stability was evaluated by comparing the response of Dihexa in stored samples with those of freshly prepared samples in acetonitrile at the same concentration.

To determine the stability of Dihexa in blood, both on ice and at 37ºC, Dihexa was spiked in into room-temperature blood, blood on ice and HPLC grade water (n=3 per time point, per treatment). The samples were placed in a hybridization oven at 37ºC or kept on ice. At 0, 3 and 24 hours, a set of samples was removed from the oven or ice and prepared for high-performance liquid chromatography as described above for plasma samples.

To determine the stability of Dihexa in urine, both at room temperature and at 4ºC, Dihexa was spiked into chilled urine and HPLC grade water (n = 3) and the samples stored at room temperature or at 4ºC for zero, 0.5, 1, 3 and 24 hours. At each time point, a set of samples was removed from the refrigerator or bench top and prepared for high-performance liquid chromatography as described above for urine samples. To determine the freeze-thaw stability of Dihexa in urine, Dihexa was spiked into chilled urine and HPLC grade water (n = 3) and the samples stored at -20ºC or at 4ºC. After 24 hours, the samples were removed from the freezer and prepared for high-performance liquid chromatography as described above for urine samples.

5.3. Results and Interpretation

5.3.1. Method Validation

5.3.1.1. Solubility

Dihexa is composed of two amino acids, one of which is relatively hydrophobic (Ile), surrounded by two hydrophobic non-amino-acid moieties. The resulting effect of these structural properties is that Dihexa is a highly water-insoluble molecule. The $logP_{OW}$ of Dihexa is estimated to be 2.24 based on software modeling (ADMET Predictor®, Simulations Plus Inc., Lancaster CA, USA). Achieving complete dissolution of Dihexa in liquids can, therefore, be challenging. To this end, we have attempted dissolution of Dihexa in a number of buffers and solvents, including varying concentrations of ethanol, acetonitrile, glycerol, propylene glycol, polyethylene glycol (200-3350), α- and β- cyclodextrins, sodium citrate solution pH 9.4, glycine buffer pH 3.0, acetic acid, dimethyl formamide and dimethyl sulfoxide. Of these, the only solutions that truly dissolved Dihexa included ≥50% acetic acid and ≥75% dimethyl sulfoxide. We therefore made all stock solutions of Dihexa by dissolving Dihexa lyophilized powder in 90-100% dimethyl sulfoxide at 1 mg/mL. This solution was then used to make serial dilutions of Dihexa in 50% dimethyl sulfoxide for samples of 100-500 µg/ml, or in HPLC grade water for samples of 50 µg/mL or less.

5.3.1.2. Selectivity and Chromatography

The method described here provided excellent separation and resolution of Dihexa and the internal standard, both in plasma and in urine. There were no interfering peaks that co-eluted with the analyte or internal standards (Figures 5.1 and 5.2). Dihexa extracted from plasma samples eluted at 7.0 minutes and the internal standard at 5.0 minutes. Dihexa extracted from urine samples eluted at 6.4 minutes and the internal standard at 8.5 minutes (the gradient was changed slightly from that used for plasma samples in order to accommodate the internal standard used for urine samples, which eluted later). Peak purity analysis revealed peak purity indexes for Dihexa and the internal standards were within the range of 0.9998-1.0.

Optimization of the mobile phase composition and gradient yielded an optimum mobile phase consisting of acetonitrile and water with 0.1% (v/v) formic acid. The addition of formic acid produced better peak shape and size than the addition of acetic or heptafluorobutyric acid, or no acid added. However, the difference between formic acid and acetic acid as an additive was negligible. Acetic acid was often used in place of formic acid since our laboratory has a large supply on hand. A number of organic phase (acetonitrile) gradients were tested, beginning with a gradient of 30 to 80% B and ending with a gradient of 23 to 30% B. The optimal gradient for separation and resolution of Dihexa and the internal standard extracted from plasma was 23 to 31% B over 9 minutes. The optimal gradient for separation and resolution of Dihexa and the internal standard extracted from urine was 23 to 35% B over 9 minutes. These methods provided optimal peak shape and separation of Dihexa and the internal standards with minimal run time.

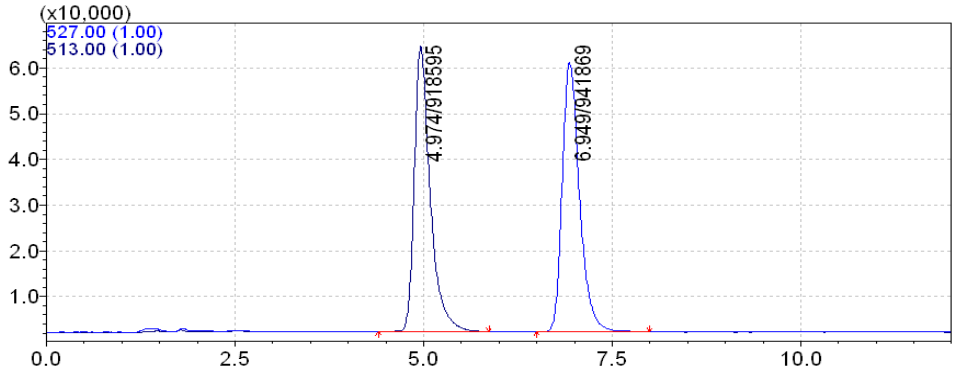

Figure 5.1 Representative chromatogram of Dihexa (m/z 527.00) and internal standard (m/z 513.00) recovered from rat blood. The chromatographic conditions consisted of an Econosphere C18 (100mm x 2.1mm) column and mobile phase consisting of acetonitrile and water with 0.1% formic acid. Separation was achieved using a gradient starting at 23% acetonitrile and increasing to 31% acetonitrile over 9 minutes at ambient temperature and a flow rate of 0.3mL/min.

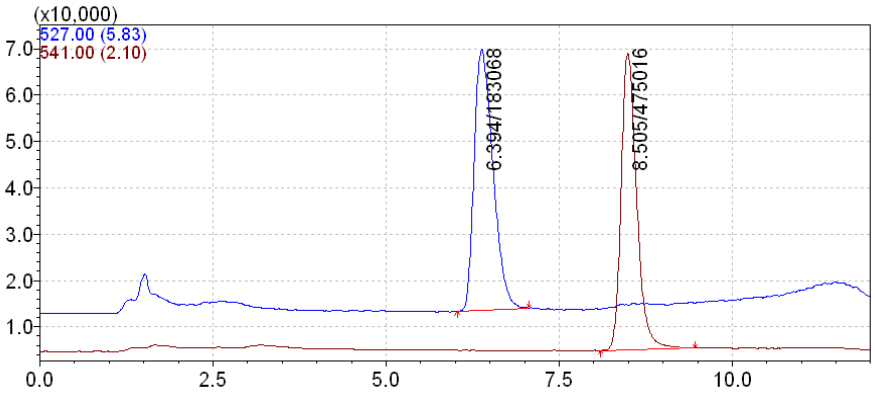

Figure 5.2 Representative chromatogram of Dihexa (m/z 527.00) and internal standard (m/z 541.00) recovered from rat urine. The chromatographic conditions consisted of an Econosphere C18 (100mm x 2.1mm) column and mobile phase consisting of acetonitrile and water with 0.1% formic acid. Separation was achieved using a gradient starting at 23% acetonitrile and increasing to 35% acetonitrile over 9 minutes at ambient temperature and a flow rate of 0.3mL/min.

5.3.1.3. Recovery

The recovery of Dihexa from blood and plasma by acetonitrile protein precipitation was evaluated using three replicate samples for each of 5 concentrations of Dihexa spiked in blood (n = 3), plasma (n = 3) or water (n = 3). Plasma was extracted from the blood samples and all of the samples were protein precipitated using acetonitrile. The samples were then transferred to autosampler vials containing two volumes of HPLC grade water. There was no apparent loss of Dihexa during sample processing. In fact, the LC/MS response for blood and plasma samples was sometimes higher than for water controls.

The recovery of Dihexa from urine by acetonitrile protein precipitation was evaluated using three replicate samples for each of 7 concentrations of Dihexa spiked in urine (n = 3) or water (n = 3) (Table 5.2). The urine samples were concentrated in a Savant SpeedVac® concentrator. Dihexa was extracted from the concentrated urine samples by protein precipitation using acetonitrile to precipitate larger urine proteins for removal from the samples, which were then transferred to autosampler vials containing two volumes of HPLC grade water. Extraction efficiency decreased with decreasing urine concentrations and ranged from 23.32% at 0.1 ug/mL to 87.04% at 100 µg/mL.

Table 5.2 Recovery of Dihexa from urine.

Dihexa Concentration (µg/mL)	% Recovery ± SD
0.1	23.45 ± 3.53
0.2	12.90 ± 3.86
1	37.13 ± 7.94
10	63.50 ± 6.04
20	75.47 ± 9.41
50	83.38 ± 8.61
100	87.65 ± 13.32

5.3.1.4. Precision and Accuracy

Table 5.3 shows within- and between-run precision and accuracy for the determination of Dihexa concentrations in plasma. The within- and between-run bias for the determination of Dihexa concentrations in plasma was less than 15%, demonstrating good accuracy for the assay. The maximum deviation of estimated values from actual values was 11.03% within-run, and 10.74% between-runs. Precision (R.S.D.) values were below 15% for, both, within-run and between-run calculation. These data indicate that the method for quantification of Dihexa concentrations in plasma samples is accurate and reproducible.

Table 5.3 Within- and between-run precision and accuracy of the assay for Dihexa in plasma (n = 3, mean ± SD).

Concentration (µg/mL)	**Precision (average ± SD)**		**Accuracy**			
	Within-run	**Between-run**	**Within-run**		**Between-run**	
			%	**Bias (%)**	**%**	**Bias (%)**
100	100.08 ± 0.10	100.06 ± 10.59	100.08	0.08	100.06	0.06
10	10.20 ± 0.18	10.29 ± 1.31	102.00	2.00	102.88	2.88
1	0.89 ± 0.05	0.89 ± 0.07	88.97	-11.03	89.26	-10.74
0.1	0.10 ± 0.01	0.09 ± 0.01	95.49	-4.51	94.88	-5.12
0.05	0.05 ± 0.00	0.05 ± 0.00	96.39	-3.61	96.27	-3.73

Table 5.4 shows within- and between-run precision and accuracy for the determination of Dihexa concentrations in urine. The within- and between-run bias for the determination of Dihexa concentrations in urine was less than 15% at concentrations between 0.1 and 100 µg/mL, demonstrating good accuracy for the assay at these concentrations. The maximum deviation of estimated values from actual values was 7.91% within-run, and 9.05% between-runs at these concentrations. Precision (R.S.D.) values were less than 15% for within-run quantification of samples of 1 to 100 µg/mL, and were within 20% at the lower limit of quantification (0.1 µg/mL). For between-run calculations R.S.D. values were between 10 and 30% for quantification of samples of 1 to 100 µg/mL, and were just under 50% at the lower limit of quantification. These data indicate that the method for within-run quantification of Dihexa concentrations from 0.1 to 100 µg/mL in urine samples is accurate and reproducible.

Table 5.4 Within- and between-run precision and accuracy of the assay for Dihexa in urine (n = 3, mean ± SD).

Concentration (µg/mL)	**Precision (average ± SD)**		**Accuracy**			
	Within-run	**Between-run**	**Within-run**		**Between-run**	
			%	**Bias (%)**	**%**	**Bias (%)**
100	100.01 ± 0.02	102.43 ± 10.36	100.01	0.01	102.43	2.43
10	10.00 ± 0.00	10.38 ± 2.36	99.99	-0.01	103.85	3.85
1	1.00 ± 0.00	1.01 ± 0.29	100.28	0.28	101.37	1.37
0.1	0.09 ± 0.02	0.09 ± 0.04	92.09	-7.91	90.95	-9.05

5.3.1.5. Curve-Fit and LLOQ

The relationships between concentration and response were fit to a Boltzmann sigmoidal equation with an r^2 value for plasma samples of ≥ 0.997 and for urine samples of ≥ 0.996. The lowest concentration that could be quantified with an average bias of 20% or less was 0.05 µg/mL for plasma samples and 0.1 µg/mL for urine samples, making these concentrations the lower limits of quantification (LLOQ).

5.3.1.6. Stability Studies

The stability of Dihexa stock solutions (DMSO/water) at 15ºC was assessed. The samples were transferred to autosampler vials and internal standard was added. The samples were stored in the autosampler and injected into the system for HPLC-MS analysis on day one, three and nine after preparation. There was no apparent reduction in response over nine days. The stability of Dihexa in acetonitrile stored at -20ºC over 64 hours was also assessed. There was no reduction in the responses compared to freshly made samples. These data indicate Dihexa is stable in its stock solution if chilled for at least nine days and in acetonitrile at -20ºC for at least two days, and probably much longer.

The stability of Dihexa in blood on ice and at 37ºC was assessed (n = 3) by comparing samples of Dihexa spiked in blood and stored on ice or at 37ºC at 0, 3 and 24 hours. The responses for these samples were normalized against the responses for control samples of Dihexa spiked in HPLC grade water and stored on ice or at 37ºC (Figure 5.3). Peak area ratios were different for blood vs. water samples because all samples were processed as described for preparation of blood/plasma samples for HPLC-MS in section 5.2.3 and recovery is slightly less for water samples processed in this way. There was no significant reduction in response for blood samples spiked with Dihexa and stored on ice, indicating that Dihexa is stable in blood on ice for at least 24 hours. There was a 6.43% reduction in response of blood samples stored at 37ºC between zero and 3 hours, and a 23.58% reduction in response between 3 and 24 hours. These data indicate that Dihexa is metabolized in the blood at 37ºC. The calculated stability $t_{1/2}$ value based on a single phase exponential decay was 10.53 hours ($r^2 = 0.98$), however this value does not represent the real biological half life of Dihexa in blood due to the fact that the curve does not extend to the point at which the blood level of Dihexa was at or near zero. Interestingly,

there was an increase in response of water samples spiked with Dihexa and stored at 37ºC. This is likely due to the fact that Dihexa is incompletely dissolved in water initially at 100µg/mL (the concentration used for all samples in this experiment), and continues to dissolve when the water is heated to 37ºC.

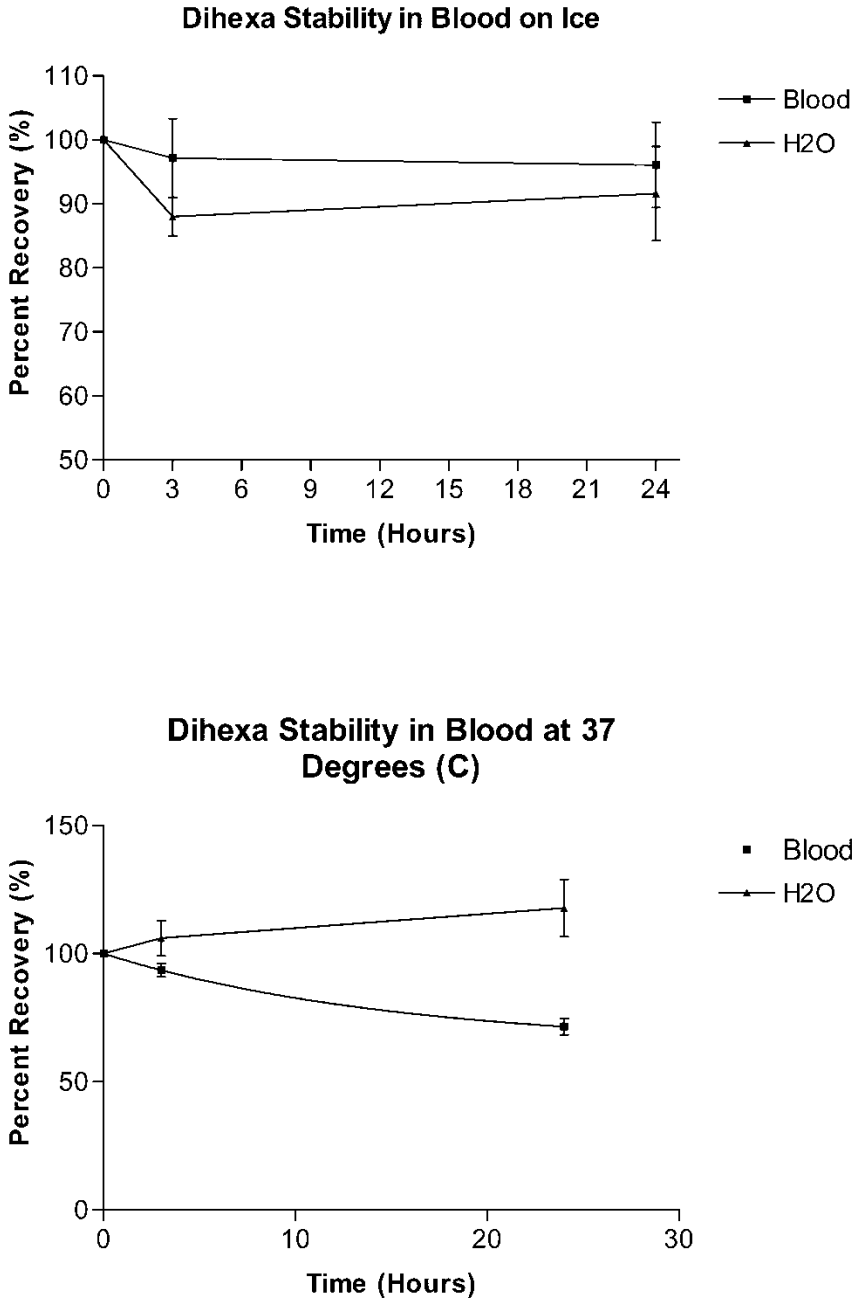

Figure 5.3 Stability of Dihexa in rat blood stored at 37º C or on ice as compared to Dihexa stored in water at 37º C on ice (n = 3). Percent recovery over time (mean ± SD).

The stability of Dihexa in urine at room temperature and at 4ºC was assessed (n = 3) by comparing samples of Dihexa spiked in urine and stored at room temperature or at 4ºC at 0, 3 and 24 hours. The responses for these samples were normalized against the responses for control samples of Dihexa spiked in HPLC grade water and stored at room temperature or at 4ºC (Figure 5.4). There was no significant reduction in response for urine samples spiked with Dihexa and stored at room temperature or at 4ºC. These data indicate that Dihexa is stable in urine at room temperature or chilled for at least 24 hours. Freeze-thaw stability of Dihexa was also tested in both urine and water with no apparent decrease in response after freezing for either group of samples (Figure 5.5).

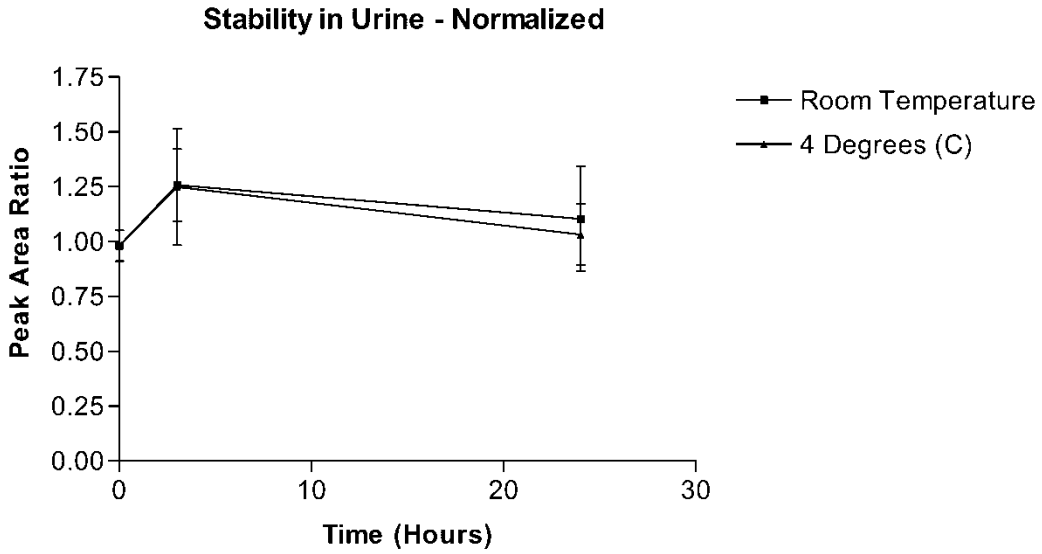

Figure 5.4. Stability of Dihexa in rat urine stored at room temperature as compared to Dihexa stored in urine at 4ºC (n = 3). Normalized against controls (Dihexa in water) (mean ± SD).

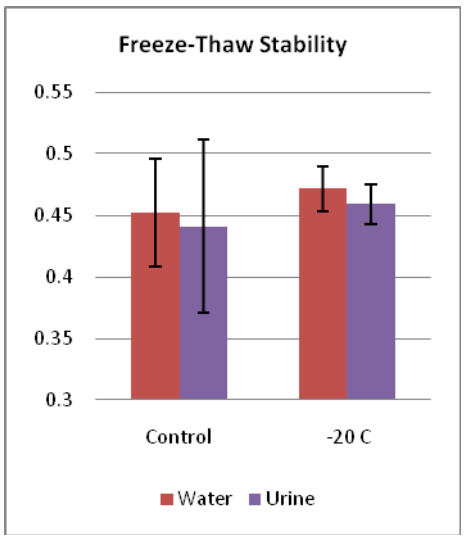

Figure 5.5 Freeze-thaw stability of Dihexa (n = 3) as measured by HPLC/MS response (mean ± SD).

5.3.2. Pharmacokinetics and Metabolism

5.3.2.1. Modeling of Physicochemical Properties

Basic physicochemical properties of Dihexa were estimated using ADMET Predictor® software (Simulations Plus Inc., Lancaster, CA, USA). This software uses algorithms to model and predict these properties based on the structure of the molecule. Though not a substitute for experimental determination, such data provides a useful estimation of these properties. Table 5.5 shows the resulting values for parameters of interest.

Table 5.5 Predicted Physicochemical Properties of Dihexa

Physicochemical Property	**Predicted Value**
logP	2.25
P_{eff}	1.78
P_{avg}	0.62
Pr_{Unbnd}	22.59

The logP value is a measure of hydrophobicity. It is the log of the octanol-water partition coefficient. A logP of 2.25 indicates that in a mixture of equal parts octanol and water, the ratio of the concentrations of Dihexa in octanol vs. water would be 177.83:1. This indicates that Dihexa is highly hydrophobic.

The values for P_{eff} and P_{avg} are predictors of permeability across gastrointestinal tract membranes. P_{eff} represents effective human jejunal permeability. A P_{eff} value of 1.78 is similar to that of caffeine (1.71) and is intermediate between that of enalapril (1.25) and piroxicam (2.14), orally administered drugs in use in the clinic that were modeled for reference. P_{avg} represents approximate average intestinal permeability along the entire human intestinal tract. The P_{avg} value of 0.62 for Dihexa was lower than that of the other orally administered drugs modeled for comparison – caffeine (3.83), carbamazepine (5.61), enalapril (1.08), and piroxicam (2.11).

Predicted plasma protein binding is represented by the Pr_{Unbnd} (percent unbound) value. The Pr_{Unbnd} value for Dihexa indicates that 22.59 percent of Dihexa is unbound to plasma proteins in circulation.

5.3.2.2. *In-vivo* Pharmacokinetics Studies

Adult male Sprague-Dawley rats were administered 10 mg/kg Dihexa intravenously for determination of Dihexa *in-vivo* pharmacokinetics. The resulting plasma concentration/time profile is shown in Figure 5.6. Dihexa exhibited rapidly decreasing plasma levels from 0 to 4 hours suggesting both distribution and elimination occur during this period. After 4 hours, the rate of clearance declined and plasma levels became more stable, exhibiting a relatively linear phase (on the log scale) suggesting a phase of pure elimination from 24 to 36 hours.

From 8.5 to 13 hours, plasma levels were lower than at 24 hours. Possible explanations for an increase in plasma concentrations at 24 hours include enterohepatic recirculation and entero-systemic recirculation, involving secretion of the compound into the stomach or gastrointestinal tract and subsequent reabsorption. Of these, enterohepatic recirculation seems the most probable. Humps in plasma concentration due to enterohepatic recirculation are usually seen within a few hours after meal times when bile containing drug is released into the duodenum and drug is reabsorbed from the intestine (Kwon 2001). Animals were allowed food after 12 hours, and the next plasma sample was taken at 24 hours. Therefore, such reabsorption, if occurring, would be likely to have occurred between 12 and 18 hours. Since no samples were taken during this time, plasma spikes that would have occurred due to enterohepatic recirculation would have been missed. Therefore we see only a subtle increase in plasma concentrations at 24 hours.

Relevant pharmacokinetic parameters of Dihexa as determined after IV dosing are summarized in Table 5.6. Plasma data was modeled by non-compartmental analysis using

WinNonlin® software. Dihexa exhibited a long elimination half-life ($t_{1/2}$) of 18,256 minutes (12.68 days). The volume of distribution (Vd) of Dihexa was 54.43 ± 25.55 L/kg indicating it is likely distributed outside the central blood compartment since the total blood volume of a 450 g rat is approximately 28 mL. Clearance of Dihexa from plasma occurred at a rate of 0.002674 ± 0.0012403 L/min/kg. The area under the curve (AUC), a measure of total drug exposure, was 4471.09 ± 2436.26 min.ug/mL.

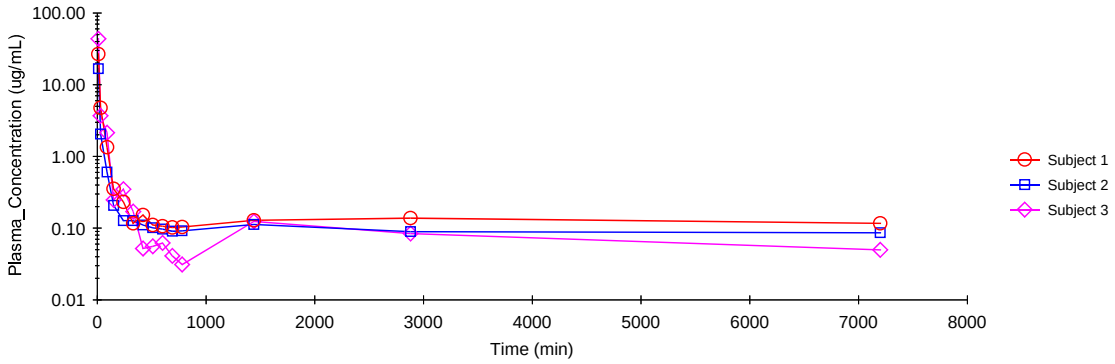

Figure 5.6 Dihexa plasma concentration vs. time curves for three rats after intravenous administration of 10 mg/kg dose in rats (n = 3).

Table 5.6. PK parameters of Dihexa following single-dose IV administration in rats.

Pharmacokinetic Parameter	**Mean**	**±**	**SD**
$AUC_{0-\infty}$ (min.μg/mL)	4471.09	±	2436.26
Vd (L/kg)	54.43	±	25.55
C_p^0 (μg/mL)	87.31	±	55.25
$t_{1/2}$ (min)	18256.48	±	13472.07
KE (min^{-1})	0.00007	±	0.00007
CL (L/min/kg)	0.002674	±	0.0012403

Five rats were administered 10 mg/kg Dihexa orally in a food-deprived state. There was no detectable Dihexa present in the resulting plasma samples. Three animals were then administered a 45 mg/kg dose orally in a fed state. The animals were sacrificed at 1, 3 and 5 hours, and 3 mL blood were taken from each. Plasma was extracted and the samples were acetonitrile protein precipitated and internal standard was added. The samples were then concentrated to a volume of 100 μL for LC/MS analysis. These samples also revealed no detectable Dihexa present.

This result was surprising given that orally administered Dihexa has significantly improved learning in rats tested in the Morris water maze task. However, *in vitro* studies have indicated that Dihexa is most effective at extremely low concentrations (unpublished data). Therefore, we postulate that Dihexa plasma concentrations after these oral administrations were simply below our limits of detection, yet were more than adequate to induce a pharmacological response. Additionally, it is likely that Dihexa is absorbed rapidly and time points at which peak

plasma concentrations occurred after 45 mg/kg dosing have been missed. This possibility is supported by a study of Dihexa pharmacokinetics after intraperitoneal dosing (reported below).

A third possibility is that Dihexa undergoes extensive first-pass metabolism resulting in extremely low plasma concentrations of the parent molecule. In this case, a metabolite of Dihexa could be responsible for its cognitive-enhancing effects. This possibility, however, is not strongly supported by results from microsomal metabolism studies (reported below), which indicated that Dihexa is not highly metabolized by phase I hepatic microsomal enzymes. It is possible that a metabolite of Dihexa after phase II metabolism is responsible for its *in-vivo* activity. This possibility has not yet been investigated by our laboratory.

A dose of 20 mg/kg Dihexa was administered to four rats intraperitoneally. The resulting plasma concentration/time profile is shown in Figure 5.7. After intraperitoneal dosing, Dihexa exhibited no obvious absorption phase in which plasma levels increased, suggesting a very rapid absorption of Dihexa from the intraperitoneal cavity into the plasma. Plasma concentrations declined rapidly from 0 to 480 minutes. At 2880 minutes, plasma concentrations decreased at a first order rate, exhibiting a linear portion of the curve (on a log scale). No obvious enterohepatic recirculation was seen after IP dosing but this could be due to the fact that the fraction of the dose reaching the plasma was low, therefore the fraction undergoing enterohepatic recirculation could be too small to be apparent.

Relevant pharmacokinetic parameters of Dihexa as determined after intraperitoneal dosing are summarized in Table 5.7. Plasma data was modeled by non-compartmental analysis using WinNonlin® software. Here, Dihexa exhibited an elimination half life ($t_{1/2}$) calculated at 12728.12 ± 6098.09 minutes. The area under the curve (AUC), a measure of total drug exposure,

was 4471.09 ± 2436.26 min.ug/mL, considerably less than the AUC calculated after IV dosing. These values were used to calculate the intraperitoneal bioavailability of Dihexa (AUC_{IP}/AUC_{IV} x $Dose_{IV}/Diose_{IP}$) at 8.32%.

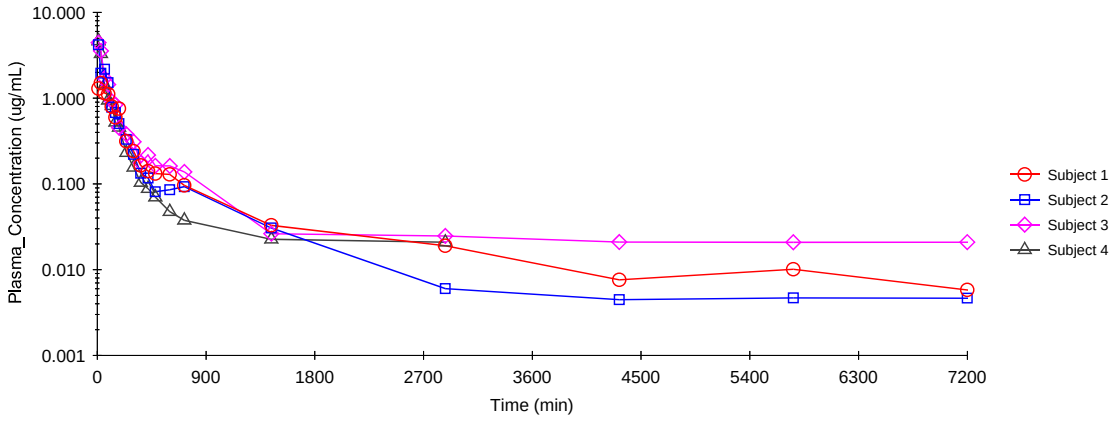

Figure 5.7 Dihexa plasma concentration vs. time curves for four rats after intraperitoneal administration of 20 mg/kg dose in rats (n = 3).

Table 5.7 PK parameters of Dihexa following single-dose IP administration in rats (n = 4).

Pharmacokinetic Parameter	**Mean**	**±**	**SD**
$AUC_{0-\infty}$ (min.µg/mL)	744.29	±	339.26
Vd (L/kg)	503.82	±	212.20
$t_{1/2}$ (min)	12728.12	±	6098.09
KE (min^{-1})	0.00007	±	0.00005
CL (L/min/kg)	0.032321	±	0.014207
F (% Bioavailability)	8.32		

Analysis of Dihexa concentrations in urine after intravenous dosing showed that the fraction of the total dose of Dihexa excreted in urine at 2160 minutes (36 hours) was 0.0747. This result suggests that renal elimination plays a minor role in the total body clearance of Dihexa. Figure 5.8 illustrates the amount remaining to be excreted and the excretion rate, alongside corresponding plasma concentrations. Figure 5.9 shows the total amount of Dihexa excreted in the urine over time. Figure 5.10 shows the rate of excretion in urine versus the corresponding plasma concentrations. This graph was linear ($r^2 = 1.00$ for average excretion rate vs. average plasma concentration), indicating linear pharmacokinetics for Dihexa.

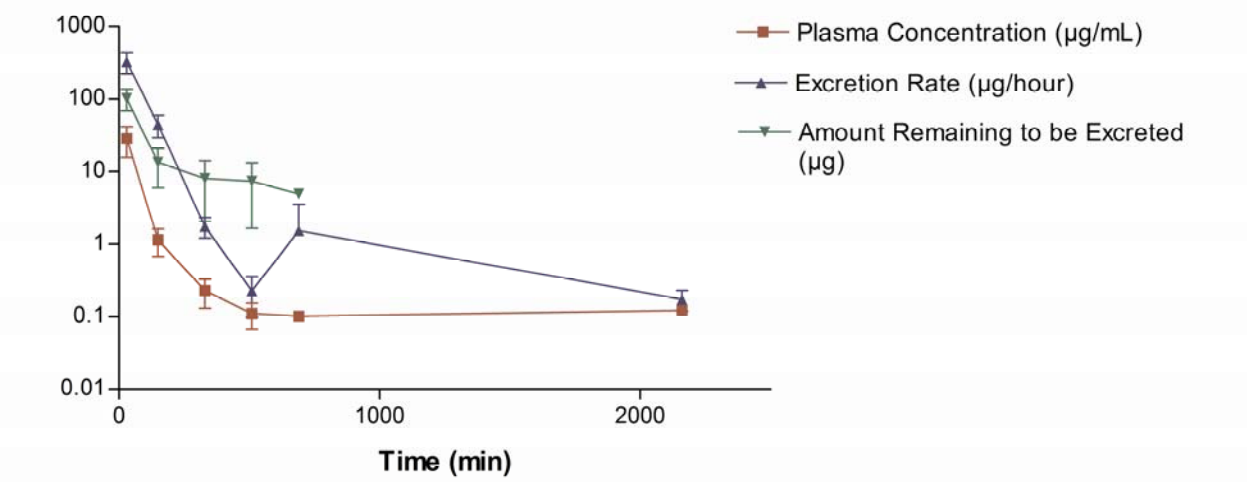

Figure 5.8. Data obtained from analysis of Dihexa concentrations in urine after a 10 mg/kg IV bolus dose. (Mean ± SD, n = 3.)

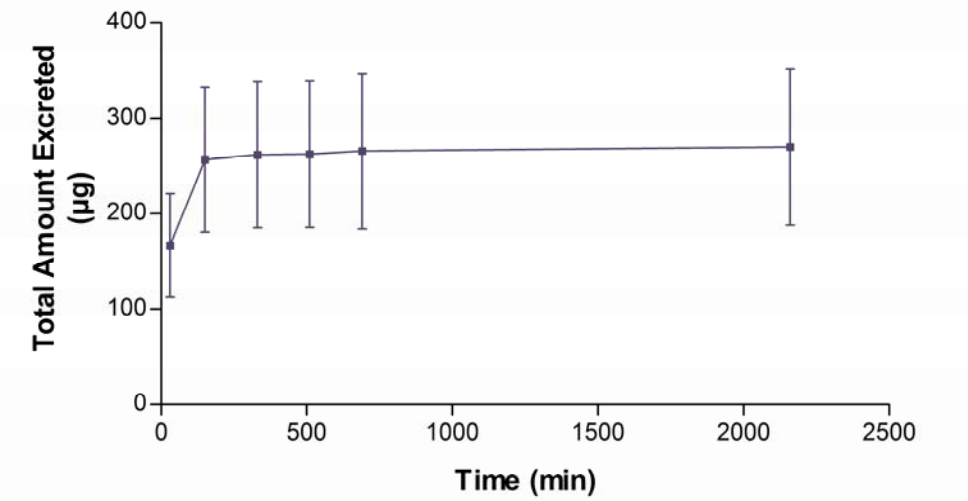

Figure 5.9. Total amount of Dihexa excreted in urine after 10 mg/kg IV bolus dose. (Mean ± SD, n = 3.)

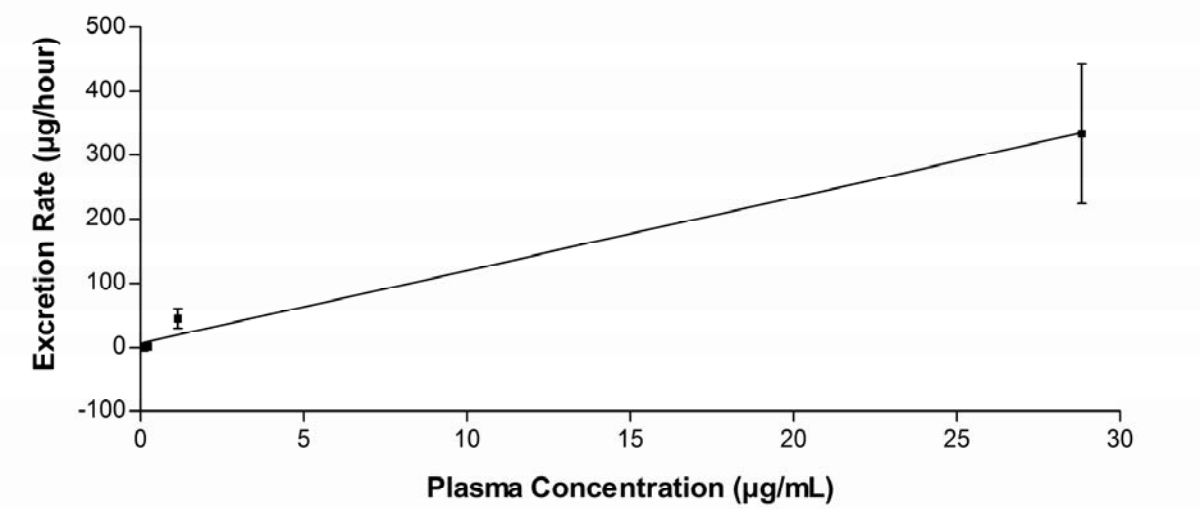

Figure 5.10. Dihexa urine excretion rate versus plasma concentration after 10 mg/kg IV bolus dose. (Mean ± SD, n = 3.)

Urine data curves after intraperitoneal dosing, including the amount remaining to be excreted, and the excretion rate, alongside corresponding plasma concentrations, are shown in Figure 5.11. Analysis of Dihexa concentrations in urine after intraperitoneal dosing showed that the fraction of Dihexa excreted in urine at 7860 minutes (131 hours) was 0.0535. The total amount of Dihexa excreted in the urine over time is shown in Figure 5.12.

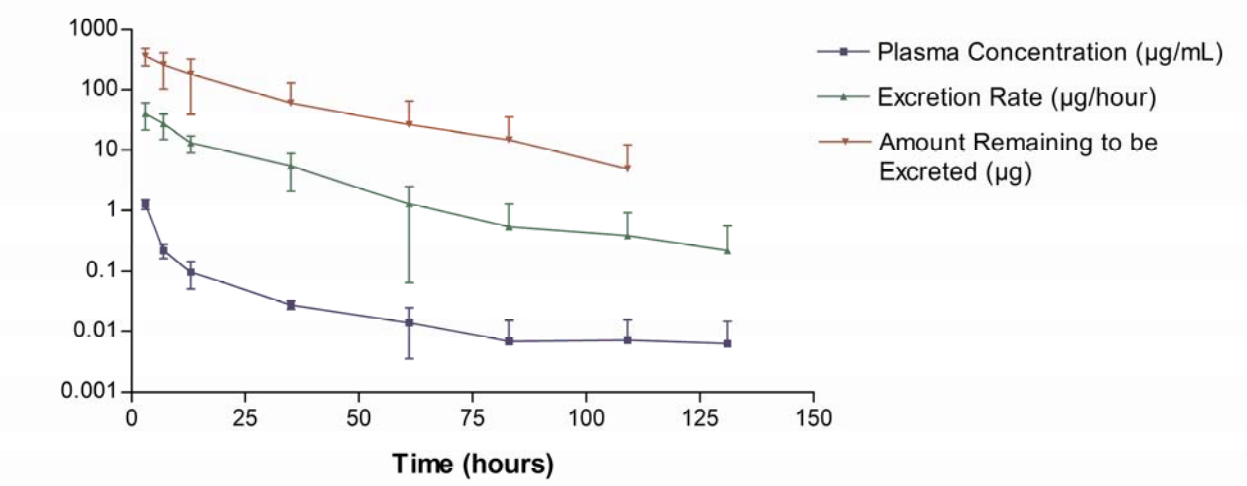

Figure 5.11 Data obtained from analysis of Dihexa concentrations in urine after a 20 mg/kg IP bolus dose. Mean ± SD, n = 5.

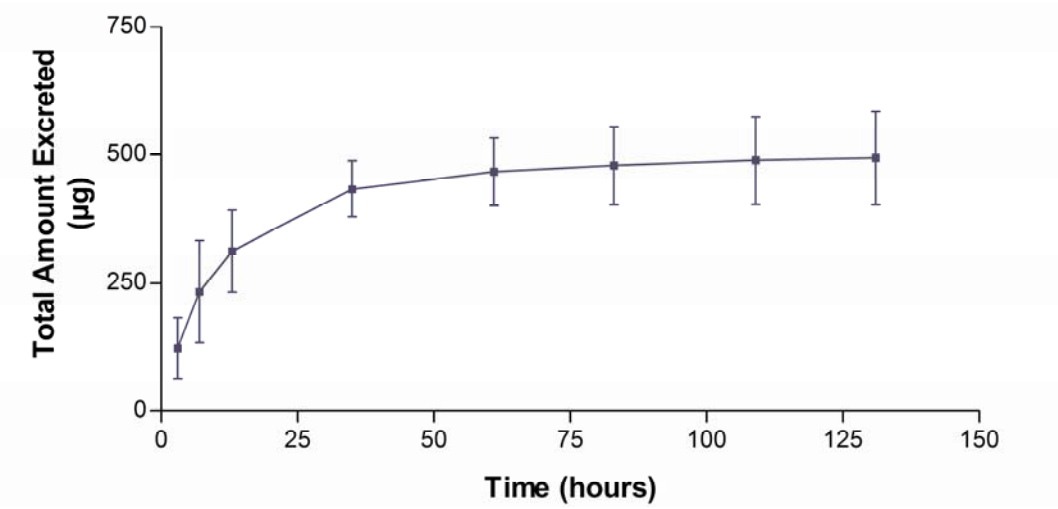

Figure 5.12 Total amount of Dihexa excreted in urine after 20 mg/kg IP bolus dose. Mean ± SD, n = 5.

5.3.2.3. Intrinsic Clearance of Dihexa in Male Rat Liver Microsomes

Phase I metabolism of Dihexa was investigated by pooled male rat liver microsomes (Figure 5.13). Dihexa exhibited an average intrinsic clearance (Cl_{int}) of 2.72 µL/min/mg, and an average half life of 509.4 minutes. The stability of piroxicam, (±)-verapamil and 7-ethoxycoumarin were also tested as high, moderate and low metabolized controls, respectively, with mean values that were within the ranges of those posted in the literature (Table 5.8) (Di 2004, Shou 2005, Lu 2006, Behera 2008). The average percent Dihexa remaining vs. time curve was fit to a one-phase exponential decay curve with an R^2 value of 0.99. These data indicate that Dihexa undergoes minimal phase I metabolism.

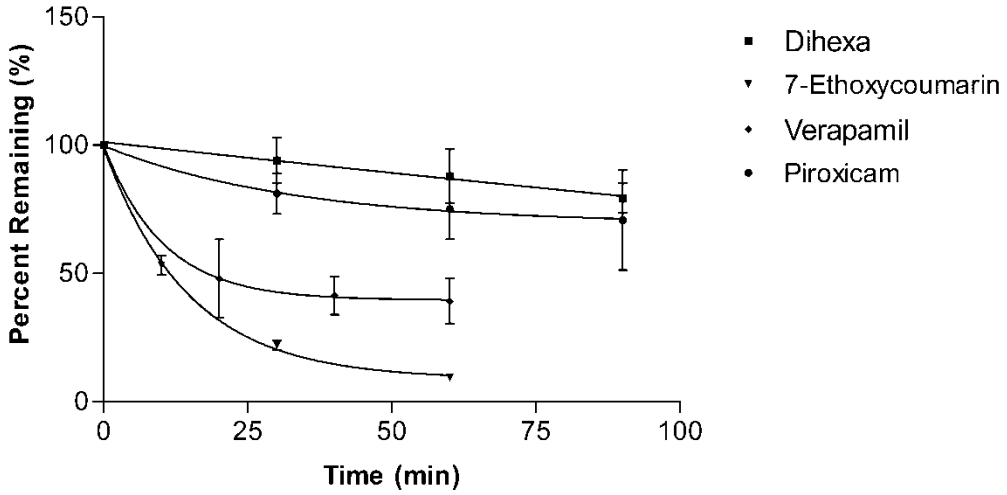

Figure 5.13 Metabolic stability profile for Dihexa, 7-Ethoxycoumarin, (±)-Verapamil and Piroxicam incubated with male rat liver microsomes (n = 3). Percent remaining over time (mean ± SE).

Table 5.8 Intrinsic clearance values for Dihexa and reference compounds (mean ± SD, n = 3 per time point per compound).

Test Compound	**Intrinsic Clearance (µL/min/mg)**
Dihexa	2.72 ± 52.90
7-Ethoxycoumarin	136.7 ± 10.17
(±)-Verapamil	112.52 ± 504.80
Piroxicam	60.22 ± 77.58

5.4. Discussion

We have presented here a simple, reproducible, accurate, and sensitive HPLC-MS assay developed for the detection and quantification of Dihexa, suitable for analysis of clinical and pre-clinical plasma or urine samples. There is currently no other assay for detection of Dihexa in plasma or urine published in the literature. This method is practical and efficient and provides a validated means of determining Dihexa concentrations in plasma and urine for our pre-clinical applications.

The validated method was used to determine the pre-clinical pharmacokinetics of Dihexa after intravenous and intraperitoneal dosing. Dihexa exhibited a long half life in-vivo compared to other angiotensin IV analogs (18,256.48 minutes based in IV dosing data) and was not cleared rapidly by the kidneys, which appear to play a minor role in the total body elimination of Dihexa based on evaluation of urine concentrations. The bioavailability of Dihexa after intraperitoneal dosing was 8.32%, suggesting that Dihexa may have undergone extensive first-pass metabolism. However this conclusion is not well supported by studies with hepatic microsomes from adult male Sprague-Dawley rats, which indicated that Dihexa is not highly metabolized by phase I metabolic enzymes. Dihexa exhibited minimal phase I enzymatic degradation compared to low, moderate and highly metabolized reference compounds. It is possible that Dihexa was extensively metabolized by phase II or other hepatic enzymes. Another possibility is that Dihexa precipitated out of solution upon injection in the intraperitoneal cavity and a large fraction of the administered dose remained within the intraperitoneal cavity.

The physicochemical properties of Dihexa were estimated using modeling software. By this estimation, Dihexa is characterized by a high logP, being highly hydrophobic. This physical characteristic is evidenced by the difficulty experienced in the laboratory solubilizing Dihexa for experimental use. Taken together with the renal clearance data, these results suggest that Dihexa may undergo renal tubular reabsorption. The glomerular filtration rate for a 500g rat is estimated to be around 3 mL/min (Rhodin 2008). The renal clearance of Dihexa is calculated to be 0.0002 L/min/kg, which extrapolates to 0.0001 L/min for a 500g rat, significantly less than 3 mL/min. Further, due to the highly lipophilic nature of Dihexa, it is likely that Dihexa tends to be retained in lipophilic membranes lining the renal tubules (Katzung 2004). Additionally, the high plasma protein binding predicted for Dihexa would also reduce the rate of renal clearance.

This idea also fits well with the moderate volume of distribution exhibited by Dihexa (54.43 L/kg based on IV dosing data), which is much greater than the total blood volume, but not nearly as large as that seen for other drugs such as PNB-0405. Such a volume of distribution might be expected from a molecule that tends to be absorbed and retained in the plasma membranes of cells in or near the vasculature. Of course, this parameter is also affected by the extent of plasma protein binding. Dihexa is predicted to be only 22.59% unbound to plasma proteins. If this is the case, plasma protein binding would also serve to decrease apparent volume of distribution.

Despite being stable against enzymatic activity and predicted to have oral bioavailability, both by software modeling and by pharmacodynamic *in-vivo* experimental data, Dihexa did not exhibit oral bioavailability in our *in-vivo* pharmacokinetic studies. Oral administration was attempted at two doses, 10 mg/kg and 45 mg/kg, the latter study done using large plasma

volumes for detection, with neither study resulting in detectable concentrations of Dihexa in the plasma. Larger doses are not feasible due to the insolubility of Dihexa until new methods of solubilizing Dihexa in physiologically inert solutions can be determined. The possible enterohepatic recirculation seen in the IV study also suggested that Dihexa might be orally bioavailable since enterohepatic recirculation would imply absorption from the gastrointestinal tract. However, enterohepatic recirculation after food intake would involve increased gastrointestinal secretions which would lower the pH, which could help solubilize Dihexa and increase its absorption across intestinal membranes.

CHAPTER SIX

DISCUSSION

Angiotensin IV is the most recently discovered and smallest member of the vasoconstriction and fluid balance-regulating family of molecules, the angiotensins. At first glance, this family of molecules seems functionally and phylogenetically far removed from oncogene product c-Met receptor and its cognate ligand hepatocyte growth factor (HGF). However, our laboratory has unveiled an interesting and ostensibly important relationship between these surprisingly related ligand-receptor systems.

In point of fact, angiotensin IV shares a partial homology with HGF and another plasminogen family member, angiostatin (Wright 2008). Specifically, angiotensin IV is homologous with the hinge (linker) region of HGF. Further, HGF/c-Met and angiotensin IV/AT_4 signaling exhibit a number of functional and signaling commonalities. In light of these shared features, our laboratory set out to investigate this relationship using angiotensin IV analogs with enhanced structural stability. As a result we have developed several synthetic analogs of angiotensin IV with agonist and antagonist activity at the AT_4/c-Met receptor(s). Using these angiotensin IV analogs, our laboratory has demonstrated a functional relationship between angiotensin IV and the HGF/c-Met receptor system by revealing the ability of angiotensin IV analogs to effect changes in c-Met receptor signaling (Yamamoto 2010).

However, ours is not the only source of evidence for functional connections between these two ligand-receptor systems. Like angiotensin IV, HGF has been shown to influence blood pressure (Biswas 2005, Vistoropsky 2008), enhance long term potentiation in the CA1 of the

hippocampus (Takeuchi 2008, Kramar 2001), and improve memory function in models of Alzheimer's disease (Olson 2004, Albiston 2004, Takeuchi 2008). Both HGF and angiotensin IV have been shown to play protective roles in endothelial function (Nakamura 1996, Morishita 1997, Wang 2004, Vinh 2008), and to promote blood flow in ischemic and normal tissues (Morishita 2002, Morishita 2004, Wright 1994, Kramar 1997). Both systems induce calcium entry into cells (Dulin 1995, Davis 2006, Tyndall 2007), and synergize with other pro-angiogenic growth factor receptor systems (Hall 1995, You 2008). Additionally, angiotensin IV has exhibited HGF-like activity in some cancers (Mustafa 2001, Ochedalska 2002). Estimated values for the size of the AT_4 receptor binding subunit (143 – 165 kDa) are close to that of c-Met's transmembrane domain (145 kDa) (Corso 2005) and one study estimated an AT_4 receptor subunit to be 50-60 kDA, similar to the extracellular domain of c-Met (50 kDa)(Corso 2005). Finally, both the c-Met and the AT_4 receptor are expressed in almost all tissues and cell types.

Our angiotensin IV analog, Norleual is a powerful antagonist of c-Met. Norleual exhibits high affinity for the c-Met receptor and potently inhibits c-Met receptor signaling and HGF-dependant cell proliferation, migration and invasion (Yamamoto 2010). Consistent with c-Met inhibition, Norleual also suppresses angiogenesis *ex-vivo* and metastasis in a murine melanoma model (Yamamoto 2010).

Chapter two of this dissertation presents the development and validation of an assay for the determination of Norleual concentrations in blood by high performance liquid chromatographic/mass spectrometry analysis. This method was demonstrated to be accurate and reproducible and thus provides a confirmed method for analysis of Norleual in blood samples.

Using this method, we were able to determine the single-dose pharmacokinetics of Norleual in rats after intravenous administration. Pharmacokinetic analysis of Norleual blood concentrations after bolus IV dosing revealed a relatively short half life (28 minutes) and low volume of distribution (1.8 L/kg). These parameters raised some concerns regarding the practical use of Norleual as a therapeutic agent. Firstly, a short half life can make maintenance of steady-state levels difficult in that frequent dosing is required. Secondly, a low volume of distribution is contradictory to permeation of the molecule deep into tissues, rather indicating that the molecule remains primarily in the circulation. This might be problematic given that Norleual is a potential anti-cancer therapeutic and may be required to reach tumor tissue that is not well supplied by the vasculature. On the other hand, this may not be an issue, and may even be beneficial, in tumors exhibiting enhanced permeation and retention, or where Norleual functions in an anti-metastatic role only.

Metabolic data obtained from rat liver microsomes indicated that Norleual may be partially metabolized hepatically. Norleual exhibited a moderate rate of metabolism by phase I enzymes compared to low, moderate and highly metabolized reference drugs. *In vitro-in vivo* correlation of microsomal and *in-vivo* pharmacokinetic data suggested that hepatic clearance is likely to be responsible for removal of Norleual that is not degraded in the blood before reaching the liver. However, experiments to assess the stability of Norleual in blood at 37º C indicated Norleual is rapidly metabolized in the blood with a half-life of 4.56 minutes. Therefore, this metabolism is likely to be the primary mechanism of clearance of Norlueal.

Correlation of predictive modeling of Norleual, using physicochemical property prediction software, with experimental data suggested that Norleual is highly bound to plasma

proteins other than albumin. Given that the isoelectric point of Norleual is estimated to be approximately 7.44, it is probable that Norleual binds to alpha-1-acid glycoprotein, a plasma protein that tends to bind cationic and neutral drugs.

Modeling of the physicochemical properties of Norleual also indicated that Norleual is slightly hydrophobic with a relatively low octanol-water partitioning coefficient (P_{ow}). This was consistent with laboratory experience handling Norleual, which dissolves in water at concentrations of 1 mg/mL and less. This characteristic is likely to be a major contributing factor to the low permeability of Norleual given that it is a small molecule at 776 Da and size should not be an inhibiting factor in its penetration of biological partitions. Hydrophilicity, along with high plasma protein binding could explain the low volume of distribution estimated for Norleual. These features of Norleual also support the predicted low oral bioavailability of Norleual by the modeling software.

With the knowledge of the limitations of Norleual's physicochemical and metabolic properties, our laboratory looked within our library of angiotensin IV analogs for molecules with chemical modifications that might resolve some of the concerns that had been raised for Norleual. One family of molecules within our library that had demonstrated potent activity at the c-Met receptor, consisted of peptidomimetics with the three c-terminal amino acids of angiotensin IV replaced by a 6-amino-hexamide moiety. Molecules in this family also contained a substitution for the valine in the first position in angiotensin IV with a norleucine with 'd,' rather than the normal 'l,' stereochemistry. These modifications at either end of the molecule were hypothesized to lend stability to the molecule by protecting it against the activities of

carboxy- and aminopeptidases. This structure describes the molecule PNB-0405, which is considered to be the parent molecule for this family of angiotensin IV analogs.

Chapter four of this dissertation describes the development of an assay for, and the determination of the pharmacokinetics of, PNB-0405. During validation, the assay demonstrated good precision and accuracy for the determination of PNB-0405 concentrations in serum ranging from 0.1 to 10 μg/mL, when using standard curve values from the same HPLC/MS run (within-run quantification). The method was less accurate for quantification of samples containing lower concentrations (0.01 μg/mL) of PNB-0405 or when using standard curve data from samples processed and run separately (between-run quantification). Less variation between values obtained from between-run quantification would be necessary in order to meet FDA guidelines for analytical method validation. However, the method demonstrated adequate accuracy for our purposes given that we always use data from standard curves processed and run simultaneously with our experimental samples. Additionally, the concentrations of our pharmacokinetic study samples fell within the range that was accurately quantifiable by the validated method.

As expected, non-compartmental pharmacokinetic analysis of serum samples obtained after intravenous and subcutaneous dosing of PNB-0405 revealed an increased half life of PNB-0405 as compared to Norleual. An increased volume of distribution was also observed. Thus, the modifications to the molecule imparted the desired changes in physicochemical and metabolic properties.

This fact was also supported by predicted values for octanol-water partitioning and oral bioavailability. PNB-0405 was predicted to be moderately hydrophobic with oral bioavailability intermediate to that of other orally administered drugs that were modeled for comparison. A lack

of phase I metabolism of PNB-0405 by rat liver microsomes was also observed, further demonstrating enhanced stability against enzymatic degradation. Experimental data revealed a plasma protein binding value of 68.49% unbound. Given that PNB-0405 possesses an isoelectric point of approximately 9.0, we estimate that, like Norleual, PNB-0405 is likely to bind primarily to alpha-1-acid glycoprotein.

These results showed that the compound PNB-0405 demonstrated desirable differences in pharmacokinetic properties as compared to Norleual. Pharmacokinetic characterization of PNB-0405 confirms the predicted outcome of the chemical modifications that were made to the angiotensin IV molecule in order to produce this more stable analog. With these data, our laboratory can now focus on identifying analogs within this family of molecules that exhibit the greatest efficacy, with a general idea of their expected pharmacokinetics.

In addition to our investigation of AT_4/c-Met receptor antagonists as potential anti-cancer therapeutics, our laboratory is also examining AT_4/c-Met receptor agonists as potential cognitive-enhancing therapeutics for the treatment of age-related dementia. One of our angiotensin IV analogs, Dihexa, has shown promising activity in this respect. Dihexa has exhibited potent activity as a c-Met receptor agonist *in-vitro* and has also proven to be highly effective at enhancing spatial learning in rats tested in the Morris water maze, both with and without chemically-induced cognitive deficits (unpublished data).

Chapter five of this dissertation describes the development and validation of a method for analysis of Dihexa in plasma and urine samples. The method showed good precision and accuracy for the quantification of Dihexa concentrations in plasma at all concentrations tested. The precision and accuracy was good for within-run quantification of Dihexa concentrations in

urine at concentrations between 0.1 and 100 µg/mL. Preferably, the assay should exhibit relative standard deviation (R.S.D.) values of less than 15% for both within- and between-run quantification, except at the lower limit of quantification where values may be within 20% R.S.D., in order to meet FDA guidelines. However, our assay met these criteria only for within-run quantification of urine samples and not for between-run quantification of urine samples. R.S.D. values were within 30% for between-run quantification of urine samples except at the lower limit of quantification. The assay was, however, acceptable for our purposes given that, as mentioned above, we always use values from standard curves that were processed and run simultaneously with our experimental samples for quantification (within-run quantification). Additionally, the assay provided a validated method of quantification of our biological samples where there existed none previously, thereby enabling us to obtain a good estimation of Dihexa pharmacokinetics.

In-vivo, Dihexa exhibited a very long half life of over 12 days. Dihexa also exhibited relative stability in blood *ex-vivo*. These results corresponded with *in-vitro* microsome study data, which indicated that Dihexa is metabolized by phase I enzymes at a very low rate, further supporting the conclusion that Dihexa is resistant to proteolytic degradation. However, the low intraperitoneal bioavailability exhibited by Dihexa suggested that Dihexa may undergo first-pass metabolism by the liver. Thus, Dihexa may be susceptible to the activities of phase II or other hepatic enzymes.

Analysis of urine Dihexa concentrations indicated that Dihexa is also cleared renally at a very low rate (0.0002 L/min/kg). The high hydrophobicity and low rate of clearance of Dihexa suggested that Dihexa may undergo tubular reabsorption in the kidneys.

Dihexa is highly hydrophobic as observed in the laboratory by its lack of solubility in many solvents, and as predicted by software modeling. Dihexa is also predicted to be mostly bound to plasma proteins in circulation. Unlike for Norleual and PNB-0405, Dihexa plasma protein binding is likely to involve primarily albumin since the isoelectric point of Dihexa is estimated to be approximately 6.46 making it slightly acidic. Hydrophobicity, acidity and degree of plasma protein binding greatly influence the volume of distribution by affecting the extent of permeation of the tissues. Dihexa exhibited a moderate volume of distribution, which was in agreement with its characterization by these properties.

Dihexa exhibited low intraperitoneal bioavailability and no oral bioavailability. This was surprising given its oral activity in behavioral studies. We hypothesize that Dihexa may be orally bioavailable to a very small degree and that resulting plasma concentrations, though below our limits of detection, are nevertheless adequate to induce a physiological response. Given that our first sample in the study using the largest dose of Dihexa was at one hour, it is possible that we have missed time points in which Dihexa concentrations were highest and might have been within our detectable range for that dose. This idea is supported by the fact that, after intraperitoneal dosing, plasma levels reached maximum concentrations within 10 minutes, indicating a very rapid absorption. It is possible that the low oral bioavailability of Dihexa can be attributed to first-pass metabolism, although this idea was not well supported by the low rate of phase I metabolism exhibited by Dihexa in the study using rat liver microsomes. However, the susceptibility of Dihexa to phase II or other metabolic enzymes has not yet been investigated.

Dihexa is probably not well absorbed in the stomach due to its tendency to be charged at the low pH within the stomach (pH 1-3). Here, Dihexa is likely to be dissolved due to a charged

state, but unable to penetrate lipid membranes. Stronger acids tend to be more absorbed in the stomach compared to weaker acids (Kwon 2001). In the intestine, where pH values are generally between 5 and 8, Dihexa is likely to be unionized, which should allow penetration of membranes there, especially given that it should be dissolved coming from the stomach. It is possible, however, that due to its high hydrophobicity, Dihexa may tend to precipitate out of solution in the intestine when its charged state is lost. Still, these properties prompt us to predict that some Dihexa should penetrate the lining of the intestine. This conclusion is supported by the appearance of enterohepatic recirculation after intravenous dosing. Gastric secretions after meals, which contribute to enterohepatic recirculation, lower intestinal pH, which may provide the right conditions for Dihexa solubility and absorption. Thus, we conclude that the fraction of Dihexa orally absorbed and transported into the systemic circulation at therapeutic doses is simply below our limit of detection.

Values for pharmacokinetic parameters varied somewhat between the intravenous and intraperitoneal dosing studies. This is likely due to the fact that neither study encompasses plasma concentrations at time points within the terminal phase encompassing an interval of more than twice the estimated half life (a rule of thumb for accurate estimation of half life and AUC) (Kwon 2001). In the case of Dihexa, this interval would have been more than 24 days. Plasma concentrations were below the limit of detection at 10 days for both studies. In order to obtain such a long terminal phase time point interval, an assay with much higher sensitivity would have to be developed. This would probably require the use of more sensitive instrumentation, such as tandem HPLC/MS/MS.

Another explanation for the differences seen between parameters obtained after intravenous and intraperitoneal dosing of Dihexa is the possible enterohepatic recycling observed after intravenous dosing. Transient increases in plasma concentrations after enterohepatic recycling could result in an underestimation of clearance (Cl). In this case clearance values estimated from urine data may be more accurate (Kwon 2001).

Future studies planned for Dihexa include investigation into the ability of the molecule to penetrate the blood-brain barrier. One of the reasons for the paucity of effective drugs for the treatment of Alzheimer's disease and other forms of age-related dementia is the difficulty of getting drugs across the blood brain barrier. The lack of active agents for treatment of dementia is not due to a lack of identifiable molecular targets but the lack of blood-brain barrier permeability exhibited by prototype molecules. As mentioned briefly above, our recent studies show that Dihexa exhibits cognitive enhancing activity when administered orally. Implicit in the manifestation of oral activity is the assumption that the molecules not only penetrate the gastrointestinal tract, but also the blood-brain barrier.

Ultimately, the goal for any potential therapeutic agent is to be successfully tested in clinical trials and introduced into the market. Before testing in human subjects can proceed, however, the potential toxicities of the compound must be ascertained. Therefore, if either Dihexa, PNB-0405 or Norleual are judged to be suitable for application to the FDA for "investigational new drug" status and advancement to clinical trials, a full panel of toxicological studies must be performed. Factors that would need to be determined include acute toxicity after a large dose, chronic toxicity occurring after multiple or chronic dosing, effects on reproductive functions and teratogenicity, carcinogenicity and mutagenicity (Katzung 2004).

Additional pharmacokinetic characterization will also be necessary for Dihexa, PNB-0405 and Norleual. For Norleual and PNB-0405, no testing has been done yet to determine potential oral bioavailability. If Norleual could be administered orally, its potential as a therapeutic agent would be much improved given that frequent dosing might not be impractical. Further study of the oral bioavailability of Dihexa is also warranted. A better understanding of the pharmacokinetics of all three molecules could also be obtained by fitting pharmacokinetic data to compartmental models. Such data would help to clarify the kinetics of delivery to target sites and enable final assessment of their potential as therapeutic agents or need for further chemical modification.

REFERENCES

Albiston AL, Pederson ES, Burns P, Purcell B, Wright JW, Harding JW, Mendelsohn FA, Weisinger RS, Chai SY. 2004. Attenuation of scopolamine-induced learning deficits by LVV-hemorphin-7 in rats in the passive avoidance and water maze paradigms. Behavioural Brain Research 154:239-243.

Allsop D, Mayes J, Moore S, Masad A, Tabner BJ. 2008. Metal-dependent generation of reactive oxygen species from amyloid proteins implicated in neurodegenerative disease. Biochemical Society Transactions 36(6): 1293-1298.

American Cancer Society. 2006. Cancer Facts and Figures 2006. Atlanta: American Cancer Society.

Behera D, Damre A, Varghese A, Addepalli V. 2008. In vitro evaluation of hepatic and extra-hepatic metabolism of coumarins using rat subcellular fractions: correlation of in vitro clearance with in vivo data. Drug Metabolism and Drug Interactions 23(3-4): 329-350.

Benvenuti S, Comoglio PM. 2007. The MET Receptor Tyrosine Kinase in Invasion and Metastasis. Journal of Cellular Physiology 213: 316-325.

Biswas P, Roy A, Gong R, Yango A, Tolbert E, Centracchio J, Dworkin LD. 2005. Hepatocyte growth factor induces an endothelin-mediated decline in glomerular filtration rate. American Journal of Physiology – Renal Physiology 288: F8-15.

Braszko JJ, Kupryszewski G, Witczuk B, Wisniewski K. 1988. Angiotensin II-(3-8)-hexapeptide affects motor activity, performance of passive avoidance and conditioned avoidance responses in rats. Neuroscience 27: 777-783.

Braszko JJ, Wlasienko J, Koziolkiewicz W, Janeck A, Wisniewski K. 1991. The 3-7 fragment of angiotensinII is probably responsible for its psychoactive properties. Brain Research 542: 49-54.

Braszko JJ, Walesiuk A, Wielgat P. 2006. Cognitive Effects Attributed to Angiotensin II may Result from its Conversion to Angiotensin IV. Journal of Renin-Angiotensin-Aldosterone System 7: 168-174.

Carlile D, Zomorodi K, Houston JB. 1997. Scaling factors to relate drug metabolic clearance in hepatic microsomes, isolated hpatocytes, and the intact liver. Drug Metabolism and Disposition 25(8): 903-911.

Caron AZ, Arguin G, Guillemette G. 2003. Angiotensin IV interacts with a juxtamembrane site on AT4/IRAP suggesting an allosteric mechanism of enzyme modulation. Regulatory Peptides 113: 9-15.

Centers for Disease Control. 2008. NCHS FASTSTATS – Leading Causes of Death. [Online]. Available from: http://www.cdc.gov/nchs/FASTATS/lcod.htm. September 30, 2008.

Centers for Disease Control. 2009. Cancer Prevention and Control. [Online]. Available from: http://www.cdc.gov/cancer/. January 8, 2010.

Coleman JK, Krebs LT, Hamilton TA, Ong B, Lawrence KA, Sardinia MF, Harding JW, Wright JW. 1998. Autoradiographic identification of kidney angiotensin IV binding sites and angiotensin IV-induced renal cortical blood flow changes in rats. Peptides 19: 269-277.

Cooper CS, Park M, Blair DG, Tainsky MA, Huebner K, Croce CM, Vande Woude GF. 1984. Molecular cloning of a new transforming gene from a chemically-transformed human cell line. Nature 311: 29-33.

Corso S, Comoglio PM, Giordano S. 2005. Cancer therapy: can the challenge be MET? Trends in Molecular Medicine 11: 284-292.

Davis CJ, Kramar EA, De A, Meighan PC, Simasko SM, Wright JW, Harding JW. 2006. AT_4 Receptor activation increases intracellular calcium influx and induces a non-N-methyl-D-aspartate dependent form of long-term potentiation. Neuroscience 137: 1369-1379

Di L, Kerns EH, Gao N, Li SQ, Huang Y, Bourassa JL, Huryn DM. 2004. Experimental design on single-time-point high-throughput microsomal stability assay. Journal of Pharmaceutical Sciences 93: 1537-1544.

Dulin N, Madhun ZT, Chang CH, Berti-Mattera L, Dickens D, Douglas JG. 1995. Angiotensin IV receptors and signaling in opossum kidney cells. American Journal of Physiology 269: F644-652.

Ebens A, Brose K, Leonardo ED, Gartz Hanson M, Bladt F, Birchmeier C, Barres BA, Tessier-Lavigne M. 1996. Hepatocyte growth factor/scatter factor is an axonal chemoattractant and a neurotrophic factor for spinal motor neurons. Neuron 17: 1157-1172.

Eder JP, Vande Woude GF, Boerner SA, LoRusso PM. 2009. Novel Therapeutic Inhibitors of the c-Met Signaling Pathway. Clinical Cancer Research 15(7): 2207-2214.

Esteban V, Ruperez M, Sanchez-Lopez E, Rodriguez-Vita J, Lorenzo O, Demaegdt H, Vanderheyden P, Egido J, Ruiz-Ortega M. 2005. Angiotensin IV activates the nuclear transcription factor-kappaB and related proinflammatory genes in vascular smooth muscle cells. Circulation Research 96(9): 965-973.

Ferri CP, Prince M, Brayne C, Brodaty H, Fratiglioni L, Ganguli M, Hall K, Hasegawa K, Hendrie H, Huang Y, Jorrn A, Mathers C, Menezes PR, Rimmer E, Scazufca M. 2005. Global prevalence of dementia: a Delphi consensus study. The Lancet 366:2112-2117.

Hall KL, Venkateswaran S, Hanesworth JM, Schelling ME, Harding JW. 1995. Characterization of a functional angiotensin IV receptor on coronary microvascular endothelial cells. Regulatory Peptides 58: 106-115.

Hamilton TA, Handa RK, Harding JW, Wright JW. 2001. A role for the angiotensin IV/AT4 system in mediating natriuresis in the rat. Peptides 22: 935-44.

Handa RK, Harding JW, Simasko SM. 1999. Characterization and function of the bovine kidney epithelial angiotensin receptor subtype 4 using angiotensin IV and divalinal angiotensin IV as receptor ligands. The Journal of Pharmacology and Experimental Therapeutics 291: 1242-1249.

Hanesworth JM, Sardinia MF, Krebs LT, Hall KL, Harding JW. 1993. Elucidation of a specific binding site for angiotensin II(3-8), angiotensin IV, in mammalian heart membranes. The Journal of Pharmacology and Experimental Therapeutics 266: 1036-1042.

Hogan DB, Bailey P, Black S, Carswell S, Chertkow H, Clarke B, Cohen C, Fisk JD, Forbes D, Man-Son-Hing M, Lanctot K, Morgan D, Thorpe L. 2008. Diagnosis and treatment of dementia: 5. Nonpharmacologic and pharmacologic therapy for mild to moderate dementia. Canadian Medical Association Journal 179(10): 1019-1026.

Honda S, Kagoshima M, Wanaka A, Tohyama M, Matsumoto K, Nakamura T. 1995. Localization and functional coupling of HGF and c-Met/HGF receptor in rat brain: implication as neurotrophic factor. Molecular Brain Research 32: 197-210.

Kadoyama K, Funakoshi H, Ohya W, Nakamura T. 2007. Hepatocyte growth factor (HGF) attenuates gliosis and motoneuronal degeneration in the brainstem motor nuclei of a transgenic mouse model of ALS. Neuroscience Research 59: 446-456.

Marum R. 2008. Current and future therapy in Alzheimer's disease. Fundamental & Clinical Pharmacology 22: 265-274.

Katzung BG. 2004. Basic and Clinical Pharmacology, Ninth Edition. New York, NY: McGraw-Hill.

Kramar EA, Harding JW, Wright JW. 1997. Angiotensin II- and IV-induced changes in cerebral blood flow. Roles of AT1, AT2, and AT4 receptor subtypes. Regulatory Peptides 68: 131-138.

Kramar EA, Armstrong DL, Ikeda S, Wayner MJ, Harding JW, Wright JW. 2001. The effects of angiotensin IV analogs on long-term potentiation within the CA1 region of the hippocampus in vitro. Brain Research 897(1-2):114-121.

Krebs LT, Kramar EA, Hanesworth JM, Sardinia MF, Ball AE, Wright JW, Harding JW. 1996. Characterization of the binding properties and physiological action of divalinal-angiotensin IV, a putative AT_4 receptor antagonist. Regulatory Peptides 67:123-130.

Knudsen BS, Vande Woude G. 2008. Showering c-MET-dependent cancers with drugs. Current Opinion in Genetics and Development 18: 87-96.

Kwon Y. 2001. Handbook of Essential Pharmacokinetics, Pharmacodynamics and Drug Metabolism for Industrial Scientists. New York, NY: Springer.

Ławnicka H, Potocka AM, Juzala A, Fournie-Zaluski MC, Pawlikowski M.2004. Angiotensin II and its fragments (angiotensins III and IV) decrease the growth of DU-145 prostate cancer in vitro. Medical Science Monitor 10(11): BR410-413.

Lee HB, Blaufox MD. 1985. Blood volume in the rat. The Journal of Nuclear Medicine 25: 72-76.

Lee J, Albiston AL, Allen AM, Mendelsohn FA, Ping SE, Barrett GL, Murphy M, Morris MJ, McDowall SG, Chai SY. 2004. Effect of I.C.V. injection of AT4 receptor ligands, NLE1-angiotensin IV and LVV-hemorphin 7, on spatial learning in rats. Neuroscience 124(2):341-349.

Lee J, Chai SY, Mendelsohn FAO, Morris MJ, Allen AM. 2001. Proteination of cholinergic transmission in the rat hippocampus by angiotensin IV and LVV-hemorphin-7. Neuropharmacology 40: 618-623.

Lu C, Li P, Gallegos R, Uttamsingh V, Xia CQ, Miwa GT, Balani SK, Gan L. 2006. Comparison of intrinsic clearance in liver microsomes and hepatocytes from rats and humans: evaluation of free fraction and uptake in hepatocytes. Drug Metabolism and Disposition 34(9): 1600-1605.

Marum RJ. 2008. Current and future therapy in Alzheimer's disease. Fundamental and Clinical Pharmacology 22: 265-274.

McCoy A, Harding JW, Wright JW. 2010. High-performance liquid chromatographic analysis of Norleual in blood. Under review for Journal of Pharmaceutical and Biomedical Analysis. (Submitted Dec. 2009).

Michieli P. 2009. Hypoxia, angiogenesis and cancer therapy: To breathe or not to breathe. Cell Cycle 8(20): 3291-3296.

Migliore C, Giordano S. 2008. Molecular cancer therapy: Can our expectation be MET? European Journal of Cancer. 44: 641-51.

Migliore C, Giordano S. 2008. Molecular cancer therapy: Can our expectation be MET? European Journal of Cancer 44: 641-651.

Morishita R, Aoki M, Nakamura S, Matsushita H, Tomita N, Hayashi S, Moriguchi A, Matsumoto K, Nakamura T, Higaki J, Ogihara T. 1997. Potential role of a novel vascular modulator, hepatocyte growth factor (HGF), in cardiovascular disease: characterization and regulation of local HGF system. Journal of Atherosclerosis and Thrombosis 4(1): 12-19.

Morishita R, Aoki M, Yo Y, Ogihara T. 2002. Hepatocyte Growth Factor as a Cardiovascular Hormone: Role of HGF in the Pathogenesis of Cardiovascular Disease. Endocrine Journal 49(3): 273-284.

Morishita R, Aoki M, Hashiya N, Makino H, Yamasaki K, Azuma J, Sawa Y, Matsuda H, Kaneda Y, Ogihara T. 2004. Safety evaluation of clinical gene therapy using hepatocyte growth factor to treat peripheral arterial disease. Hypertension 44(2): 203-209.

Mustafa T, Chai SY, Mendelsohn FA, Moeller I, Albiston AL. 2001. Characterization of the AT(4) receptor in a human neuroblastoma cell line (SK-N-MC). Journal of Neurochemistry 76: 1679-1687.

Nakamura Y, Morishita R, Nakamura S, Aoki M, Moriguchi A, Matsumoto K, Nakamura T, Higaki J, Ogihara T. 1996. A Vascular Modulator, Hepatocyte Growth Factor, Is Associated with Systolic Pressure. Hypertesion 28: 409-413.

Naritomi Y, Terashita S, Kimura S, Suzuki A, Kagayama A, Sugiyama Y. 2001. Prediction of human hepatic clearance from in vivo animal experiments and in vitro metabolic studies with liver microsomes from animals and humans. Drug Metabolism and Disposition 29: 1316-1324.

Ochedalska AL, Rebas E, Kunert-Radek J, Fournie-Zaluski MC, Pawlikowski M. 2002. Angiotensins II and IV stimulate the activity of tyrosine kinases in estrogen-induced rat pituitary tumors. Biochemical and Biophysical Research Communications 297: 931-933.

Olson ML, Olson EA, Qualls JH, Stratton JJ, Harding JW, Wright JW. 2004. Norleucine^{1}-Angiotensin IV alleviates mecamylamine-induced spatial memory deficits. Peptides 25:233-241.

Paul M, Mehr A, Kreutz R. 2006. Physiology of Local Renin-Angiotensin Systems. Physiological Reviews 86: 747-803.

Pederson ES, Harding JW, Wright JW. 1998. Attenuation of scopolamine-induced spatial learning impairments by an angiotensin IV analog. Regulatory Peptides 74: 97-103.

Pilar Carrera M, Ramirez-Exposito MJ, Duenas B, Dolores Mayas M, Jesus Garcia M, De la Chica S, Cortes P, Ruiz-Sanjuan M, Martinez-Martos JM. 2006. Insulin-regulated aminopeptidase/placental leucil aminopeptidase (IRAP/P-LAP) and angiotensin IV-forming

activities are modified in serum of rats with breast cancer induced by N-methyl-nitrosourea. Anticancer Research 26: 1011-1014.

Rhodin MM, Anderson BJ, Peters AM, Coulthard MG, Wilkins B, Cole M, et al. 2008. Human renal function maturation -- a quantitative description using weight and postmenstrual age. Pediatric Nephrology. 24(1): 67-76.

Shou WZ, Magis L, Li AC, Naidong W, Bryant MS. 2005. A novel approach to perform metabolite screening during the quantitative LC-MS/MS analyses of in vitro metabolic stability samples using a hybrid triple-quadrupole linear ion trap mass spectrometer. Journal of Mass Spectrometery 40: 1347-1356

Singleton PA, Salgia R, Moreno-Vinasco L, Moitra J, Sammani S, Mirzapoiazova T, Garcia JGN. 2007. CD44 Regulates Hepatocyte Growth Factor-mediated Vascular Integrity. The Journal of Biological Chemistry 282: 30643-30657.

Sun W, Funakoshi H, Nakamura T. 2002. Localization and functional role of hepatocyte growth factor (HGF) and its receptor c-Met in the rat developing cerebral cortex. Molecular Brain Research 103: 36-48.

Takeo S, Takagi N, Takagi K. 2007. Ischemic brain injury and hepatocyte growth factor. Journal of the Pharmaceutical Society of Japan 127(11):1813-1823.

Takeuchi D, Sato N, Shimamura M, Kurinami H, Takeda S, Shinohara M, Suzuki S, Kojima M, Ogihara T, Morishita R. 2008. Alleviation of Abeta-induced cognitive impairment by ultrasound-mediated gene transfer of HGF in a mouse model. Gene Therapy 15: 561-571.

Takiuchi S, Mannami T, Miyata T, Kamide K, Tanaka C, Kokubo Y, Koyama Y, Inamoto N, KIatsuya T, Iwai N, Kawano Y, Ogihara T, Tomoike H. 2004. Identification of 21 single nucleotide polymorphisms in human hepatocyte growth factor gene and association with blood pressure and carotid atherosclerosis in the Japanese population. Atherosclerosis 173: 301-307.

Tchekalarova J, Georgiev V. 2005. Angiotensin peptides modulatory system: how is it implicated in the control of seizure susceptibility? Life Sciences 76(9): 955-970.

Toda N, Ayajiki K, Okamura T. 2007. Interaction of endothelial nitric oxide and angiotensin in the circulation. Pharmacological Reviews 59: 54-87.

Toschi L, Janne PA. 2008. Single-Agent and Combination Therapeutic Strategies to Inhibit Hepatocyte Growth Factor/MET Signaling in Cancer. Clinical Cancer Research 14: 5941-6.

Trapp T, Kogler G, El-Khattouti A, Sorg RV, Besselmann M, Focking M, Buhrle CP, Trompeter I, Fischer JC, Wernet P. 2008. Hepatocyte growth factor/c-MET axis-mediated tropism of cord

blood-derived unrestricted somatic stem cells for neuronal injury. Journal of Biological Chemistry 283(47): 32244-32253.

Tulasne D, Foveau B. 2008. The shadow of death on the MET tyrosine kinase receptor. Cell Death and Differentiation 15: 427-434.

Tyndall SJ, Patel SJ, Walikonis RS. 2007. Hepatocyte growth factor-induced enhancement of dendritic branching is blocked by inhibitors of N-methyl-D-aspartate receptors and calcium/calmodulin-dependant kinases. Journal of Neuroscience Research 85(11): 2343-2351.

Tyndall SJ, Walikonis RS. 2007. Signaling by hepatocyte growth factor in neurons is induced by pharmacological stimulation of synaptic activity. Synapse 61(4): 199-204.

Vinh A, Widdop RE, Drummond GR, Gaspari TA. 2008. Chronic angiotensin IV treatment reverses endothelial dysfunction in ApoE-deficient mice. Cardiovascular Research 77: 178-187.

Vistoropsky Y, Trofimov S, Malkin I, Kobyliansky E, Livshits G. 2008. Genetic and environmental determinants of hepatocyte growth factor levels and their association with obesity and blood pressure. Annals of Human Biology 35: 93-103.

Wang Y, Ahmad N, Wani MA, Ashraf M. 2004. Hepatocyte growth factor prevents ventricular remodeling and dysfunction in mice via Akt pathway and angiogenesis. Journal of Molecular and Cellular Cardiology 37: 1041-1052.

Wayner MJ, Armstrong DL, Phelix CF, Wright JW, Harding JW. 2001. Angiotensin IV enhances LTP in rat dentate gyrus in vivo. Peptides 22(9):1403-1414.

Wright JW, Miller-Wing AV, Shaffer MJ, Higginson C, Wright DE, Hanesworth JM, Harding JW. 1993. Angiotensin II(3-8) [ANG IV] hippocampal binding: potential role in the facilitation of memory. Brain Research Bulletin 32: 497-502.

Wright JW, Harding JW. 1994. Brain angiotensin receptor subtypes in the control of physiological and behavioral responses. Neuroscience and Biobehavioral Reviews 18(1): 21-53.

Wright JW, Harding JW. 1997. Important roles for angiotensin III and IV in the brain renin-angiotensin system. Brain Research Reviews 25: 96-124.

Wright JW, Stubley L, Pederson ES, Kramar EA, Hanesworth JM, Harding JW. 1999. Contributions of the Brain Angiotensin IV-AT_4 Receptor Subtype System to Spatial Learning. The Journal of Neuroscience 19(10):3952-3961.

Wright JW, Harding JW. 2004. The brain angiotensin system and extracellular matrix molecules in neural plasticity, learning and memory. Progress in Neurobiology 72:263-293.

Wright JW, Yamamoto BJ, Harding JW. 2008. Angiotensin receptor subtype mediated physiologies and behaviors: new discoveries and clinical targets. Progress in Neurobiology 84: 157-181.

Yamamoto BJ, Elias PD, Masino JA, Hudson BD, McCoy A, Anderson ZJ, Varnum MD, Sardinia MF, Wright JW, Harding JW. 2010. The angiotensin IV analog Nle-Tyr-Leu-Ψ-(CH2-NH2)3-4-His-Pro-Phe (Norleual) can act as a Hepatocyte Growth Factor/c-Met inhibitor. Journal of Pharmacology and Experimental Therapeutics. (Accepted for Publication).

You W-K, McDonald DM. 2008. The hepatocyte growth factor/c-Met signaling pathway as a therapeutic target to inhibit angiogenesis. BMB Reports. 41: 833-9.

Zhang JH, Stobb JW, Hanesworth JM, Sardinia MF, Harding JW. 1998. Characterization and purification of the bovine adrenal angiotensin IV receptor (AT4) using [125I]benzoylphenylalanine-angiotensin IV as a specific photolabel. Journal of Pharmacology and Experimental Therapeutics 287(1): 416-424.

Zhang JH, Hanesworth JM, Sardinia MF, Alt JA, Wright JW, Harding JW. 1999. Structural Analysis of Angiotensin IV Receptor (AT_4) from Selected Bovine Tissues. Journal of Pharmacology and Experimental Therapeutics 289(2): 1075-1083.

Zhang L, Himi T, Morita I, Murota S. 2000. Hepatocyte Growth Factor Protects Cultured Rat Cerebellar Granule Neurons From Apoptosis Via the Phosphatidylinositol-3 Kinase/Akt Pathway. Journal of Neuroscience Research 59: 489-496.